





Review

# Catalytic Upgrading of Clean Biogas to Synthesis Gas

Nicola Schiaroli <sup>1,\*</sup> , Martina Battisti <sup>2</sup>, Patricia Benito <sup>2,\*</sup> , Giuseppe Fornasari <sup>2</sup>, Amalio Giovanni Di Gisi <sup>1</sup>, Carlo Lucarelli <sup>1,\*</sup>  and Angelo Vaccari <sup>2</sup> 

<sup>1</sup> Dipartimento di Scienza e Alta Tecnologia, Università dell'Insubria, Via Valleggio 9, 22100 Como, Italy; agdigisi@studenti.uninsubria.it

<sup>2</sup> Dipartimento di Chimica Industriale "Toso Montanari", Università di Bologna, viale del Risorgimento 4, 40136 Bologna, Italy; martina.battisti3@studio.unibo.it (M.B.); giuseppe.fornasari@unibo.it (G.F.); angelo.vaccari@unibo.it (A.V.)

\* Correspondence: nicola.schiaroli@uninsubria.it (N.S.); patricia.benito3@unibo.it (P.B.); carlo.lucarelli@uninsubria.it (C.L.)

**Abstract:** Clean biogas, produced by anaerobic digestion of biomasses or organic wastes, is one of the most promising substitutes for natural gas. After its purification, it can be valorized through different reforming processes that convert CH<sub>4</sub> and CO<sub>2</sub> into synthesis gas (a mixture of CO and H<sub>2</sub>). However, these processes have many issues related to the harsh conditions of reaction used, the high carbon formation rate and the remarkable endothermicity of the reforming reactions. In this context, the use of the appropriate catalyst is of paramount importance to avoid deactivation, to deal with heat issues and mild reaction conditions and to attain an exploitable syngas composition. The development of a catalyst with high activity and stability can be achieved using different active phases, catalytic supports, promoters, preparation methods and catalyst configurations. In this paper, a review of the recent findings in biogas reforming is presented. The different elements that compose the catalytic system are systematically reviewed with particular attention on the new findings that allow to obtain catalysts with high activity, stability, and resistance towards carbon formation.

**Keywords:** biogas; syngas; CO<sub>2</sub> valorization; dry reforming; steam reforming; bimetallic catalysts; Ni catalysts; structured catalysts



**Citation:** Schiaroli, N.; Battisti, M.; Benito, P.; Fornasari, G.; Di Gisi, A.G.; Lucarelli, C.; Vaccari, A. Catalytic Upgrading of Clean Biogas to Synthesis Gas. *Catalysts* **2022**, *12*, 109. <https://doi.org/10.3390/catal12020109>

Academic Editors: Rei-Yu Chein and Wei-Hsin Chen

Received: 21 December 2021

Accepted: 16 January 2022

Published: 18 January 2022

**Publisher's Note:** MDPI stays neutral with regard to jurisdictional claims in published maps and institutional affiliations.



**Copyright:** © 2022 by the authors. Licensee MDPI, Basel, Switzerland. This article is an open access article distributed under the terms and conditions of the Creative Commons Attribution (CC BY) license (<https://creativecommons.org/licenses/by/4.0/>).

## 1. Introduction

Six years after the Paris Agreement, the first legally binding global climate change deal, countries were asked to revise their plans for reducing emissions [1]. Since the commitments pledged in 2015 have not been sufficient for limiting global warming within 1.5 °C, and less than a decade is left to prevent irreversible damage from climate change, the Conference of the Parties held in Glasgow (COP26) was called to negotiate new pressing goals to tackle the issue [2]. With COP26 the world has had its best last chance to ensure that runaway climate change is under control. One-hundred-and-fifty-three countries have updated or drafted new emission targets, with over 85% of global emissions that are now covered by net zero commitments [3].

By now, the role of CO<sub>2</sub> as a greenhouse gas (GHG) and its impact on the environment is generally acknowledged, and many actions have been taken in the past few years to reduce CO<sub>2</sub> emissions. On the other hand, CH<sub>4</sub> has an estimated global warming potential around 30 times greater than CO<sub>2</sub> [4], which in 2016 contributed for the 17.3% of global emissions [5]. At least 25% of the warming experienced today is driven by CH<sub>4</sub> from human actions [6]. However, its role in climate change has only received the deserved recognition during COP26. The pledge to reduce global methane emission by 30% by 2030 that has been signed during the negotiations will prevent more than 8 Gtons/year of CO<sub>2</sub> equivalents from reaching the atmosphere [3,7]. As a matter of fact, specialists from all over the globe agree that reducing CH<sub>4</sub> emissions is the single most effective strategy to keep the goal of

limiting warming to 1.5 °C within reach [6,8,9]. The major sources of CH<sub>4</sub> include enteric fermentation associated with cattle population; distribution, transmission, and storage of natural gas; and decomposition of wastes in landfills [10]. Every year, human activities produce over 105 billion tons of organic wastes, emitting methane. Their recycling through anaerobic digestion by the biogas industry has the potential to reduce the worldwide GHG emissions by 10 vol.% by 2030 [11].

In this framework, biogas (BG) seems to provide an answer to both the problem of methane emission of organic waste and landfills and to the need for decarbonization, being a renewable alternative to fossil-based resources. It is then clear why in the last 20 years BG has become the object of an impressive number of studies, going from about a hundred publications in the year 2000 to 3358 in 2020 (Figure 1). Nevertheless, in 2019, BG accounted for only 1% of the total gross inland energy consumption worldwide, and in the same year Europe consumed an amount of BG only equivalent to the 4% of natural gas consumption. This demonstrates that, up to now, BG is not a readily available alternative to fossil gas, thus its promotion through financial support and technological developments is fundamental and compelling [12].

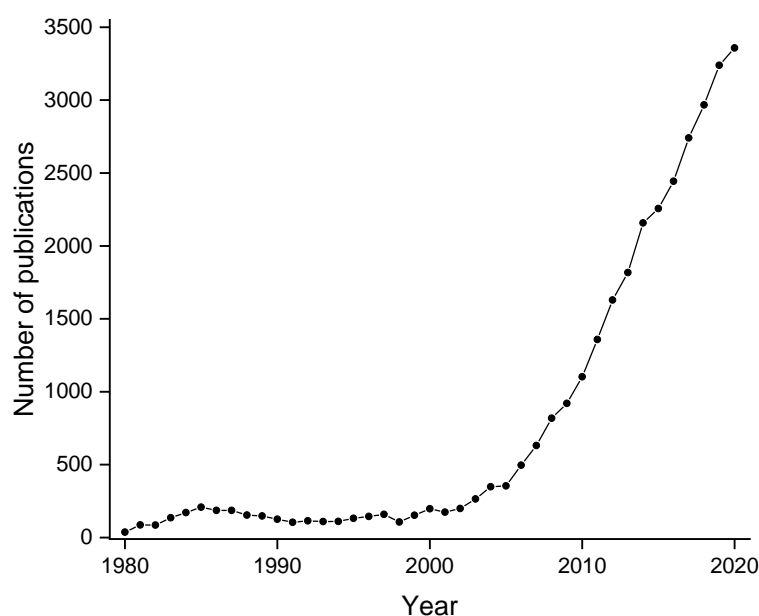


**Figure 1.** Number of publications containing the word “biogas” in the title, abstract or keywords from 1980 to 2020 found on the Scopus database.

### *Biogas*

BG is a complex mixture of methane (50–70% vol.%), carbon dioxide (30–50% vol.%) and other components in trace amount, such as water, hydrogen sulfide, siloxanes, volatile organic compounds (VOCs), ammonia, oxygen, carbon monoxide and nitrogen [13]. Its production relies on the anaerobic digestion of different types of biomasses, ranging from urban organic waste, industrial wastewater, plants and animal industry by-products, and dedicated crops. Then, the resulting BG is purified from the contaminants, such as sulfur and nitrogen compounds [14] and utilized in different applications, depending on the level of purification. The most straightforward use is its combustion for heating and lightning purposes, principally carried out at household levels and in rural areas of developing countries [15]. However, the major BG application is in combined heat and power systems (CHP), converting almost one-third of the produced BG in Europe. This method relies on the use of biogas in an electricity generating system without wasting the heat produced through combustion, which is used for space or water heating, industrial processes, greenhouses, etc. [16–18].

Another application of BG under study is the generation of electricity at high temperatures or by using a catalytical system in fuel cells. However, high capital costs and long start-up times are the principal drawbacks in this kind of application [15,19]. By analyzing the literature, it is possible to highlight that the energy balance (sum of thermal and electrical energy generated through CHP system—sum of thermal and electrical energy used in the anaerobic digestion (AD) treatment) seems advantageous, nevertheless, it is important to consider that the above results convey only an energy balance while the effective environmental impact is not directly considered [20–29].

In addition to these direct applications for green energy production, BG could be upgraded to biomethane (BM) using a variety of techniques (water scrubbing, physical or chemical absorption, pressure swing adsorption, membrane separation, cryogenic separation) [30].

Currently, 10 vol.% of the BG produced in Europe is upgraded to BM [16]. Although efficiency values are close to 100%, upgrading biogas, strictly from an energy perspective, seems to be non as convenient, since there would be an overall energy loss that can be prevented by burning biogas as it is. On the other hand, for BM to be injected in the natural gas (NG) grid or to be used as a fuel of various kinds, upgrading it to BM is the ideal path, assuring high CH<sub>4</sub> purity and high energy efficiencies. To better understand whether the BM may represent an environmentally friendly alternative, it is important to compare the impact of its production and use to the one associated with the exploitation of NG [31–35].

The highest global warming potential (GWP) in BM production is obtained when energy crops are used due to the employment of agricultural machinery, herbicides, etc. [36]. The GWP is reduced when BM is produced from wastes such as municipal solid wastes, agro-industrial wastes and manures, reaching negative values when BM leakage from storage is avoided. By comparing the results, it is possible to conclude that, on the basis of the GWP values, the production of BM may be considered environmentally attractive only in very few cases. Its production seems to be advantageous only if obtained from urban or agro-industrial wastes. To accurately evaluate the overall effect on the environment, it is therefore important to point out all the parameters involved in the production and utilization of BG or BM that could be considered as a possible source of impact [37–39].

Lastly, BG could also be chemically upgraded to high added value products, such as syngas (a mixture of CO and H<sub>2</sub>) or hydrogen, through reforming reactions (Figure 2). Syngas, in turn, has many applications such as producing methanol or long-chain hydrocarbons via the Fischer–Tropsch process.

Many studies in the last decade report encouraging results about the transformation of biogas into hydrogen or syngas. The first step for the upgrading of BG to chemicals is the production of syngas that represents the starting point to produce hydrogen, methanol and hydrocarbons. The H<sub>2</sub>/CO ratio mainly depends on the reforming technology used.

Steam Reforming (SR):  $\text{CH}_4 + \text{H}_2\text{O} \rightleftharpoons \text{CO} + 3\text{H}_2$

Partial Oxidation (PO):  $\text{CH}_4 + 0.5\text{O}_2 \rightarrow \text{CO} + 2\text{H}_2$

Dry Reforming (DR):  $\text{CH}_4 + \text{CO}_2 \rightleftharpoons 2\text{CO} + 2\text{H}_2$

Combined Steam/Dry reforming of Biogas (S/DR):  $2\text{CH}_4 + \text{CO}_2 + \text{H}_2\text{O} \rightleftharpoons 3\text{CO} + 5\text{H}_2$

Water Gas Shift (WGS):  $\text{CO} + \text{H}_2\text{O} \rightleftharpoons \text{CO}_2 + \text{H}_2$

Methane Dry reforming (MTR): a combination of SR, PO and DR.

Autothermal Reforming (ATR): a combination of SMR and PO

In fact, when syngas is obtained with a suitable H<sub>2</sub>/CO ratio, it can be processed in a water gas shift (WGS) section to obtain pure hydrogen or it can be transformed in methanol or in hydrocarbons by Fischer–Tropsch process [40,41]. BG can be used as such (after purification) or after CO<sub>2</sub> removal as BM. If BM is considered as feedstock to produce syngas, it is easy to understand that the current technology can be applied, instead, if BG is the starting feed, the reforming unit must be opportunely modified to maximize the CO<sub>2</sub> conversion. By analyzing the existing literature, it is possible to state that there is the possibility to convert biogas into syngas with different H<sub>2</sub>/CO ratios by tuning the operation conditions and by using an appropriate catalyst. Starting from

these assumptions, it is fundamental to evaluate whether the use of BG instead of the NG represents a sustainable route to produce syngas.

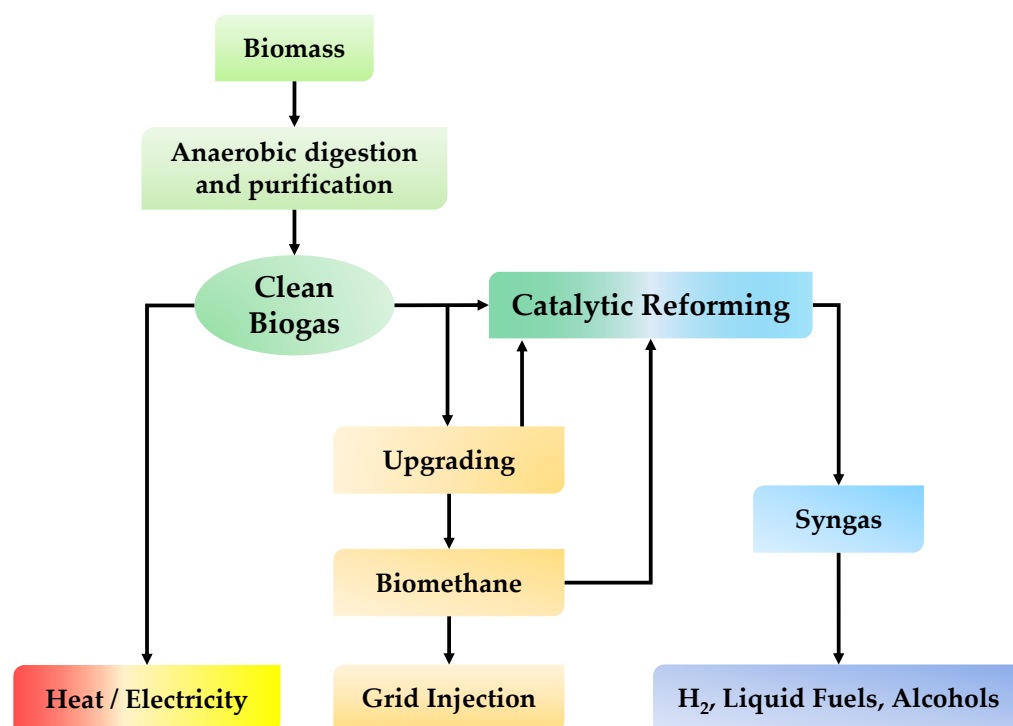


**Figure 2.** Biogas utilization routes.

The Life Cycle Assessment (LCA) studies found in the literature report result in comparing different ways to convert BG or BM into different chemicals. In this way, it is possible to state which route is most appealing for the conversion of this feedstock, but it is impossible to verify whether BG could represent a suitable alternative to natural gas. Analyzing the GWP for the production of H<sub>2</sub> starting from BG or BM, the impact of the production of a certain amount of hydrogen depends on the feed used and the technology applied for biogas upgrading [42–46].

The synthesis of methanol using BG seems to be more attractive from an environmental point of view if compared to H<sub>2</sub> production. Additionally, in this case, it is possible to assert that the impact is a function of the feedstock used for the production of BG and the technology used for its upgrade [47–52]. Recently, Schiaroli et al. [53] reported a study in which both BG and NG are considered as feed for the production of syngas (suitable for methanol synthesis). As reported above, syngas represents an intermediate to produce methanol, hydrogen, and hydrocarbons. Considering that the current technologies for the production of these chemicals are very similar, the syngas production may be taken into account to carry out representative LCA studies. As reported in the above cited manuscript, the production of syngas starting from BG instead of NG is environmentally convenient only using the combined steam and dry reforming technology and simultaneously utilizing BG as an energy supplier.

Summarizing the findings reported in this paragraph, it seems that the use of BG as a feedstock to produce chemicals may represent an alternative to the NG. It is noteworthy that most of the authors report comparison between different upgrading technologies and not a comparison between BG and NG, avoiding highlighting whether this renewable source can represent an alternative to the fossil fuels.

In any case, it is fundamental to realize a solid process in which the choice of the best catalytic system determines both the economic and the environmental sustainability.

## 2. Catalysts for Biogas Upgrading

### 2.1. Monometallic Ni-Based Catalysts

The reforming of BM has been performed using different classes of catalyst containing different active phases and support. Starting from studies conducted on the well-known steam reforming of NG, and considering the low price and the fact that they are easy to synthesize, Ni-based catalysts have been widely investigated not only in presence of steam but also for the dry reforming of BG [54–60]. The choice of Ni as active phase for the upgrade of BG to syngas using dry or combined reforming may represent an economic alternative to noble and more expensive metals (Figure 3) but the overall catalytic formulation could be carefully modulated to obtain a performing and stable material.

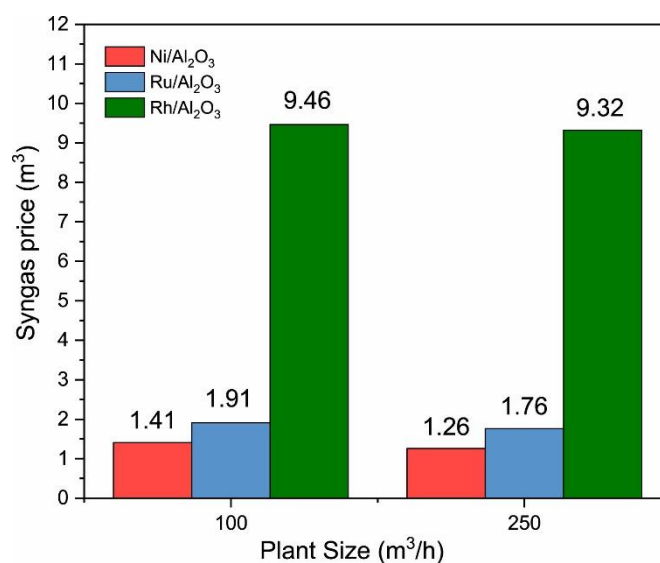
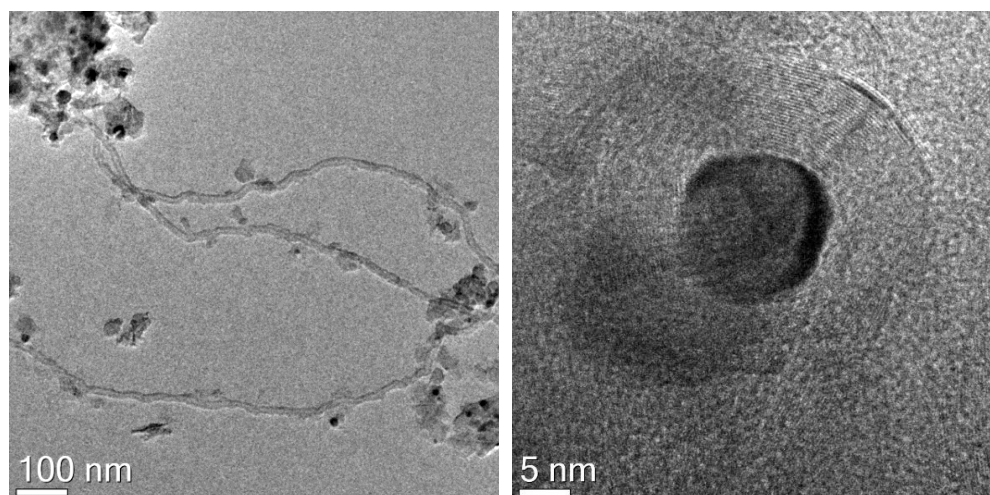


Figure 3. Estimated prices of syngas using different catalysts [30].

The catalysts can be synthesized using different synthetic routes such as: impregnations [61–65]; one-pot evaporation-induced self-assembly [66]; template-free (TF) synthesis followed by hydrothermal treatment [67]; sol-gel synthesis [68–70]; preparation from hydrotalcite-type precursors [71,72]; pH-controlled impregnation [73]. Alumina or Mg/Al/O mixed oxides are widely used as support for Ni-based catalysts for their thermal stability. Several papers report on the behavior of this class of materials. Ni/Al<sub>2</sub>O<sub>3</sub> catalysts showed good performances in terms of CH<sub>4</sub> conversion (98% when H<sub>2</sub>O/CH<sub>4</sub> is 6.1), also at 600 °C cofeeding a large amount of water; CO<sub>2</sub> in these conditions showed very low conversion (23% when H<sub>2</sub>O/CH<sub>4</sub> = 1.2) [74]. Other authors investigated alumina as support in steam and dry reforming of biogas finding high methane and CO<sub>2</sub> conversions and syngas produced with interesting H<sub>2</sub>/CO values with temperatures ranging from 600 to 900 °C [66,73,75–83]. It has been demonstrated that 5 wt.% Ni supported on microporous alumina is more active and resistant compared to the 5 wt.% Ni supported over nonporous alumina. The interaction between active phase and support strongly increases in case of samples synthesized introducing the active phase precursor at the beginning of the synthesis process, leading the formation of more resistant catalysts [66]. The distribution of the Ni particle on the alumina surface plays a fundamental role on the activity and stability of these catalysts also in DR of BG. A more efficient synthesis allowing the formation of highly dispersed and reducible Ni particles that increase the activity of samples [73]. It is noteworthy that the reoxidation of Ni<sup>0</sup> may take place in steam reforming conditions, while a strong deactivation caused by a massive coke formation is observed during dry reforming (Figure 4) [70,74–76,83].



**Figure 4.** TEM images of typical carbonaceous materials formed during dry reforming: carbon nanotubes (**left**) and encapsulating carbon (**right**).

The addition of Mg to the catalytic formulation leads to the formation of mixed spinel phases and basic sites that have been proven to improve the CO<sub>2</sub> conversion and the overall stability [75,76,83]. Depending on the synthetic routes, the interaction, and the dispersion of Ni<sup>0</sup> over the support could be increased allowing the increases in both activity and resistance to coke formation [77,84–88]. Silica has also been investigated as a possible support for Ni in dry and combined reforming. Samples containing the same amount of Ni and prepared using the same procedure show different behaviors in methane dry reforming and silica SBA-15 resulted to be more active and stable (CH<sub>4</sub> and CO<sub>2</sub> conversion of 78% and 85%, respectively) than aerosol and diatoms [61]. Although using silica as a support facilitates the reduction in Ni species, weak interaction between active phase and support causes rapid deactivation (from 90% to 80% for both CH<sub>4</sub> and CO<sub>2</sub> after 100 h of reaction at 750 °C) [89]. High surface area values and the possibility to obtain support with a specific lattice structure have been claimed as the responsible for the performances of Ni/SBA-15, Ni/MCM41 or other amorphous silica supports [60,88,90–94]. Good results in dry, combined and tri-reforming of methane have also been obtained with Ni/ZrO<sub>2</sub> catalysts well-known to be stable at high temperatures [88,95–98]. A non-innocent support has been identified into CaO that can be synthesized in different ways showing different physical properties such as surface area, porosity, and crystallite size. Ni supported over these materials showed interesting activity that resulted higher for the sample obtained by hard template synthesis with an initial value of 80% for both CH<sub>4</sub> and CO<sub>2</sub> conversion [67]. The possibility to modulate the acidity and basicity of the samples is one of the reasons for the choice of the hydroxyapatite as support for Ni and other metals active in the dry reforming of BG. It has been noted that samples containing 10 wt.% of Ni increase their activity during time-on-stream; ascribed by the authors to the evolution of active surface that promote the activation of Ni<sup>2+</sup> cations inserted to the apatitic structure and, on the other hand, the formation of Ni<sup>0</sup> particles on top of carbon nanofibers that results active in the dry reforming of methane (CH<sub>4</sub>, CO<sub>2</sub> conversion = 35%, 45% at 700 °C, 1.6 bar) [99]. Similar results have been reported by several authors, highlighting the possibility to use this class of materials as possible candidates for the production of stable catalysts for dry reforming of methane or BG [100,101]. The possibility to regenerate the above-cited group of catalysts demonstrated by Rego de Vesconcelos et al. [102] is noteworthy, as it represents a remarkable upgrading in the DR processes.

## 2.2. Metal Oxides as Activity Promoters

Ni-based catalysts can be improved by different promoters and supports that enhance its performance, stability, and resistance to carbon formation in the reforming harsh reaction

conditions.  $\text{CeO}_2$  has been successfully applied in dry, steam reforming and combined processes [103–106]. The redox chemistry between  $\text{Ce}^{3+}$  and  $\text{Ce}^{4+}$ ,  $\text{CeO}_2$  high oxygen affinity and adsorption/excitation energy bands associated with its electronic structure, together with its Lewis acid and base sites, makes ceria a suitable promoter to suppress carbon formation on the catalyst surface.  $\text{Ni}/\text{CeO}_2$  catalysts were reported to be active in reforming reactions and activate  $\text{CO}_2$  [107,108].  $\text{CeO}_2$  is reduced by  $\text{H}_2$  in the reaction and the oxygen can be replenished by  $\text{CO}_2$ . Carbon dioxide can be then converted to  $\text{CO}$  while the adsorbed oxygen is available to provide a pathway for carbon oxidation. As demonstrated by Al-Swai et al. [109], a  $\text{CeO}_2$ - $\text{MgO}$  binary oxide (15:85 wt/wt) can improve Ni activity in the DR at low temperature. The authors report that, although further improvements are needed regarding the stability of the catalyst, a 20 wt.%  $\text{Ni}/\text{CeO}_2$ - $\text{MgO}$  catalyst shows remarkable  $\text{CH}_4$  and  $\text{CO}_2$  conversions at 400 °C (20%, GHSV = 36,000  $\text{mL g}^{-1} \text{h}^{-1}$ ), higher than those registered for similar catalysts tested at higher temperatures [110,111]. On the other hand, carbon more likely forms at such high Ni loading, and this aspect can be detrimental to the achievement of an optimal compromise between quantity of active sites and resistance to carbon deactivation, especially at low reaction temperature.

The type of synthesis can highly influence either the  $\text{CeO}_2$  promotion or the reaction pathways. Das et al. [112] reported the utilization of a new core-shell structured  $\text{Ni-SiO}_2@/\text{CeO}_2$  catalyst for the dry reforming reaction at 600 °C. The final catalyst was composed of nanometric spheres in which the porous  $\text{Ni/SiO}_2$  surface is covered by a uniform thin layer of  $\text{CeO}_2$  (~10 nm). This catalyst configuration increases the Ni dispersion and reducibility as well as the resistance to agglomeration, thus avoiding deactivation over 72 h. The results in terms of activity and carbon formation were compared to the bare  $\text{Ni-SiO}_2$  system and a  $\text{Ni-CeO}_2$  catalyst obtained through impregnation. Though there was a clear occurrence of the RWGS reaction ( $\text{H}_2/\text{CO}$  ratio ~0.5 mol/mol), the  $\text{Ni-SiO}_2@/\text{CeO}_2$  showed a superior carbon oxidation capacity (0.047  $\text{gC/g}_{\text{catalyst}}$  after 72 h) due to the synergic  $\text{Ni-CeO}_2$  interaction that, as evidenced by in situ DRIFTS analysis, surprisingly changed the dry reforming reaction pathway (Figure 5).

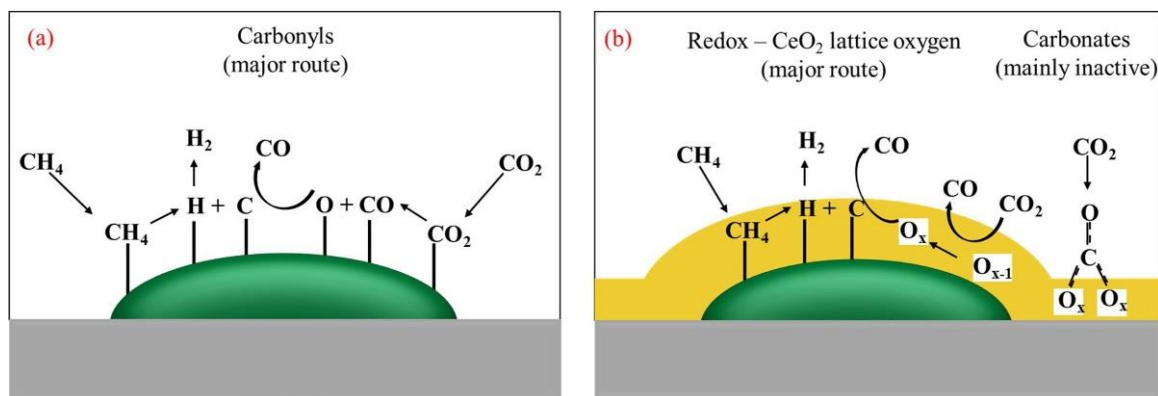


**Figure 5.** Mono-functional and Bi-functional reaction mechanism for dry reforming on (a)  $\text{Ni-SiO}_2$  and (b)  $\text{Ni-SiO}_2@/\text{CeO}_2$  catalyst. Reprinted with permission from [112]. Copyright (2018) Elsevier.

Similar results were obtained from Marinho et al. [113] for  $\text{Pt@CeO}_2$  and  $\text{Pt@CeZrO}_2$ . The formation of an embedded structure enhances the extent of ceria reduction and the creation of oxygen vacancies on the catalyst surface. DRIFTS revealed the formation of carbonates only for the embedded catalysts and not for a traditional  $\text{Pt}/\text{CeO}_2$  system, evidencing a higher amount of oxygen vacancies over these structures.

$\text{Ni-CeO}_2$  catalysts were also applied in combined steam and dry reforming in a recent work by Gao et al. [114]. A ZSM-5 support was chosen to deposit  $\text{Ni-CeO}_2$  because of its unique textural and physicochemical properties. From the results, the use of ZSM-5 allowed to obtain a high specific surface area of 286  $\text{m}^2/\text{g}$  and microporous structure that improves the metal-support interaction and help to increase the resistance to deactivation.

The Ni and Ce loading show that both the elements have crucial effects on the catalyst performances. The tuning of CeO<sub>2</sub> amount can increase the catalytic activity and stability in both terms of CH<sub>4</sub> and CO<sub>2</sub> conversion. The optimal catalyst composition is 20 wt.% of Ni and 2 wt.% of Ce, attaining conversion of CH<sub>4</sub> and CO<sub>2</sub> of 95% and 85%, respectively, at 800 °C, 0.5 of steam-carbon ratio and 3.6 L h<sup>-1</sup> g<sup>-1</sup>. This catalyst was stable over 40 h of reaction with a total amount of carbon deposited lower than 5% of the catalyst weight.

Other rare earth oxides were reported to be promising promoters for reforming reactions. Among them, Lanthanum oxide, if used as a support in dry reforming reaction, can effectively activate CO<sub>2</sub>, reducing the deposition of carbon by enhancing its oxidation [115,116]. Charisiou and co-workers [117] studied the BG reforming over a Ni/La<sub>2</sub>O<sub>3</sub>-ZrO<sub>2</sub>. The catalyst showed a high dispersion of La<sub>2</sub>O<sub>3</sub> in the ZrO<sub>2</sub> lattice and TEM analyses revealed the presence of cubic Zr<sub>0.9</sub>La<sub>0.1</sub>O<sub>1.95</sub>. The investigation of surface basicity by CO<sub>2</sub>-TPD experiments revealed that the La-modified catalyst presents a high population of very strong basic sites that can efficiently activate CO<sub>2</sub> and enhance carbon gasification. It is noteworthy that it was found that these properties could also enhance the occurrence of RWGS reaction, which lowered the H<sub>2</sub>/CO ratio of the reforming outlet stream but increasing the CO<sub>2</sub> conversion in all reaction conditions tested.

Similar catalysts were applied in the steam reforming of methane and model BG at low temperature to produce H<sub>2</sub>. This process aims to produce pure hydrogen at temperatures of 400–550 °C, which offers the chance to remarkably lower the operating costs, in addition to favoring the WGS reaction in a one-step reactor. These features could be limited by thermodynamic constraints that required the use of hydrogen-selective membrane and the use of a highly active catalyst to shift the chemical equilibrium towards H<sub>2</sub>. Angeli et al. [118] synthesized the catalysts via wet impregnation of Ni or Rh on La<sub>2</sub>O<sub>3</sub>-CeO<sub>2</sub>-ZrO<sub>2</sub> and La<sub>2</sub>O<sub>3</sub>-ZrO<sub>2</sub> supports. ZrO<sub>2</sub> can enhance the accumulation of water on the surface to form hydroxyl groups at 500 °C [119] while La improves the oxygen storage-capacity and thermal stability of CeO<sub>2</sub>-ZrO<sub>2</sub> [120]. Rh enhances the presence of oxygen vacancies over the reducible support through the spillover effect, while Ni has a minor influence on the support reducibility. This behavior, already observed in previous works [121–125], increases the resistance of the Rh catalyst towards carbon formation, but it was probably responsible for surface modifications during the time on stream, which caused a mild deactivation of 16.7% after 60 h of reaction. Hence, the choice of a Ni 10 wt.% CeZrLa catalyst was the best in terms of stability and activity even when the reforming of biogas was conducted at 7 bar, 500 °C, GHSV of 30,000 h<sup>-1</sup> and a S/CH<sub>4</sub> of 3. In these conditions, the CH<sub>4</sub> conversion values over 90 h of time on stream reach the thermodynamic equilibrium (~18%). Although the carbon formation through Boudouard reaction can be fast in the low temperature range, the authors observe low carbonaceous material accumulation, which is highly reactive towards oxidation or hydrogenation.

Perovskites containing Ni/La and other elements such as Co [126], Rh [127], Sr [128], Fe [129], Zn [130], Ce [131] and Ca [132], were successfully applied in BG reforming. The general formula of these compounds is ABO<sub>3</sub>, where A is an alkaline earth metal or a rare earth element, while B is a 3d transition metal. By partially substituting the site A or B it is possible to tune different properties of the catalyst such as the oxygen mobility/vacancies, its redox behavior, and the oxidation state of the elements, which influence the catalytic activity and stability of the material.

By adding Mn and Co to LaNiO<sub>3</sub> perovskite structure, Kim et al. [133] were able to obtain a highly active tri-metallic LaNi<sub>0.34</sub>Co<sub>0.33</sub>Mn<sub>0.33</sub>O<sub>3</sub> catalyst for DR of BG (CH<sub>4</sub>/CO<sub>2</sub> = 1 mol/mol). The results suggested that the superior performance may come from a closer interaction between Ni and La<sub>2</sub>O<sub>3</sub>, mediated by MnO that, together with Co, stabilized the Ni particles avoiding their detachment and the further polymerization of carbon over the support (Figure 6).



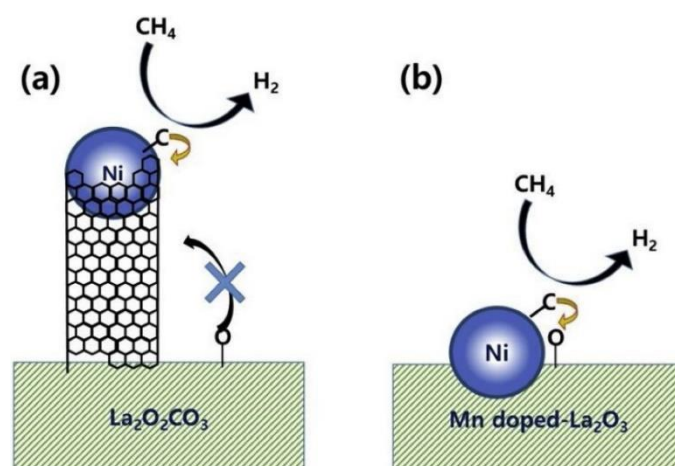


**Figure 6.** (a) Nickel nanoparticles detach from support by filamentous carbon that block oxygen supply to metal surface. (b) The metal nanoparticles are in close contact with the support and receive oxygen supply to produce CO. Reprinted with permission from [133]. Copyright (2019) Elsevier.

While the application of such systems in dry reforming reaction may be easily found in the literature, there are few works regarding their application in combined steam and dry reforming. In this context, Yang et al. [134] studied the promotional effect of strontium on the performance of a Ni/La perovskite oxide. After the synthesis of the catalysts with different amounts of Sr ( $\text{La}_{1-x}\text{Sr}_x\text{NiO}_3$ ,  $x = 0-0.5$ ), the systems were tested in the steam reforming of biogas ( $\text{CH}_4/\text{CO}_2 = 1$  mol/mol), focusing the attention particularly on the structure and resistance of the catalyst towards carbon deposition. It was reported that the Sr concentration influences the properties of the catalyst. Firstly, due to differences in  $\text{Sr}^{2+}$  and  $\text{La}^{3+}$  ionic radii, the generation of different perovskite phases after calcination can be detected. The presence of this element lowered the catalytic activity, but greatly suppressed the formation of carbon during reaction. It was stated that the Sr species generated during reforming homogeneously covered the catalyst surface, accelerating the activation of  $\text{CH}_4$  and  $\text{CO}_2$ . The  $\text{La}_{0.9}\text{Sr}_{0.1}\text{NiO}_3$  catalyst showed great stability for 20 h of reaction, reaching conversions of  $\text{CH}_4$  and  $\text{CO}_2$  of 83% and 70%, respectively, at 900 °C and  $\text{S}/\text{CH}_4$  of 0.5 mol/mol.

Although generally used to promote the activity of Cu in WGS [135] and Methanol synthesis [136], ZnO was also applied in biogas valorization through reforming [137,138]. A study by Cunha and co-workers [139] examined the performance of a zeolite 13X doped with Ni-ZnO in the combined reforming of BG for the syngas production in a wide range of reaction temperatures using a feed of  $\text{CH}_4:\text{H}_2\text{O}:\text{CO}_2$ , in a molar ratio of 3:2:1. In this work, a new type of pre-treatment was proposed; before the tests, the catalyst was exposed to a gas stream of CO at 400 °C for 2 h. The main idea was to exploit Boudouard's reaction to enrich the catalyst surface in filamentous carbon that, detaching the Ni particles from the support, would decrease the sintering phenomena easily occurring during reaction. The results showed that although the Ni crystal sizes were relatively large, the Ni-ZnO/13X shows the best performance reaching the total  $\text{CH}_4$  valorization at 800 °C and  $\text{CO}_2$  conversion of almost 55%. In a recent work by Chatla et al. [140], the Zn effect on a NiMgAl mixed oxide catalyst for dry reforming reaction was investigated. To do so, hydrotalcite-type precursors with different Zn loadings were obtained by co-precipitation, maintaining a constant 10 wt.% Ni loading in the final catalyst. The reduction behavior of the catalysts (Figure 7) shows that by increasing the amount of Zn, the reducibility of the catalyst increases as weaker metal-support interactions predominate, while the NiO-ZnO interaction become stronger.

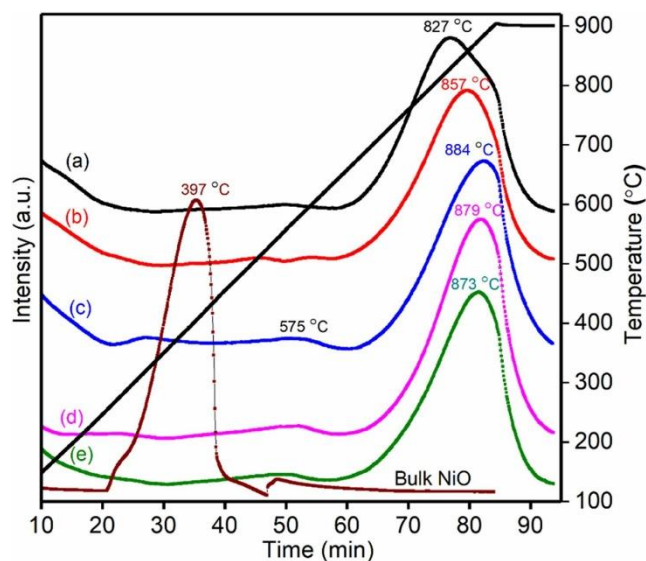


**Figure 7.** Effect of ZnO loading on NiO reducibility. H<sub>2</sub>-TPR profiles of (a) NiMgAl, (b) NiMgAl-1Zn, (c) NiMgAl-3Zn, (d) NiMgAl-5Zn, (e) NiMgAl-10Zn catalysts. Reprinted with permission from [140]. Copyright (2022) Elsevier.

ZnO acts as a booster of basicity, that enhances CO<sub>2</sub> adsorption and activation as well as the occurrence of reverse Boudouard's reaction. Interestingly, the XPS analyses of the reduced samples show different shifts of both Ni and Zn binding energies, strongly suggesting the formation of a Ni-Zn alloy on the catalyst surface. All these features promote the catalytic activity in DR, showing a clear improvement in performance especially when Zn concentration is 3 wt.% (0.115 mol<sub>CH<sub>4</sub></sub> min<sup>-1</sup> g<sub>Ni</sub><sup>-1</sup> vs. 0.098 mol<sub>CH<sub>4</sub></sub> min<sup>-1</sup> g<sub>Ni</sub><sup>-1</sup> of NiMgAl sample). Moreover, the Zn-doped catalyst shows fewer and shorter carbon nanotubes after 100 h of reaction and a narrower distribution of the active phase with an average size of Ni particles of 10 nm. This evidences the promoting effect of Ni-Zn alloy formation, in line with a similar work on Ni-Zn systems [141].

Having been recently reported as catalysts for CO<sub>2</sub> activation, In and In<sub>2</sub>O<sub>3</sub> [142–144], were studied as promoters of the Ni activity in dry reforming. A Ni-In/CeO<sub>2</sub>-Al<sub>2</sub>O<sub>3</sub> catalyst [145] was successfully applied at low temperature DR (650 °C), showing CH<sub>4</sub> and CO<sub>2</sub> conversions of 37% and 25%, respectively. The addition of 0.3 wt.% of In via deposition-precipitation stabilizes the activity of a 3 wt.% Ni/Al<sub>2</sub>O<sub>3</sub> catalyst and decreases carbon formation, avoiding the increase in the reactor pressure drop. Since the average size of the reduced particles was found to be independent from the catalyst composition, the reason behind In promotion was suggested to be of electronic nature. The authors stated that In plays a double role as CeO<sub>2</sub> modifier, promoting the formation of a higher number of Ce<sup>3+</sup> sites after reduction, and increasing the Ni performance by an alloy formation. The long-term stability of a Ni-In based catalyst for dry reforming was assessed by Liu et al. [146], who prepared a series of confined Ni-In intermetallic alloy nanocatalysts (In<sub>x</sub>Ni@SiO<sub>2</sub>) via a one-pot method using the bimetallic nanoparticles as cores and porous SiO<sub>2</sub> as shell. TEOS was used as silica precursor. The Ni content was fixed at 7 wt.%, while the amount of In was varied in the range 0.0–7.0 wt.%. The catalysts screening at variable temperatures (550–800 °C, 1 bar, CH<sub>4</sub>:CO<sub>2</sub> = 1:1 and GHSV of 18,000 mL h<sup>-1</sup>g<sub>cat</sub><sup>-1</sup>) shows that both CH<sub>4</sub> and CO<sub>2</sub> conversion decreased with the In content. From the apparent activation energy calculations, it turns out that the addition of In has an insignificant influence on CO<sub>2</sub> activation, while CH<sub>4</sub> is hardly dissociated when In concentration increases (81 kJ mol<sup>-1</sup> without In, up to 101 kJ mol<sup>-1</sup> for In<sub>1.0</sub>Ni@SiO<sub>2</sub>). On the other hand, a low CH<sub>4</sub> activation energy would lead to a quick and higher carbon deposition, evidencing that this parameter must be finely tuned to have optimum compromise between catalytic activity and carbon adsorption. In this sense, In can effectively weaken carbonaceous deposition,

but at the expense of a lower  $\text{CH}_4$  conversion rate. The  $\text{In}_{0.5}\text{Ni@SiO}_2$  is able to resist to the deactivation over 430 h of DR reaction ( $\text{CH}_4$  and  $\text{CO}_2$  conversion of 90% and 95%, respectively) showing a coke formation that is negligible for the first 20 h. In this sense, the confinement of the nanoparticles inside the silica shell (Figure 8) further provided higher resistance towards both sintering and coke formation, as demonstrated by comparison with a supported Ni-In/ $\text{SiO}_2$  catalyst.

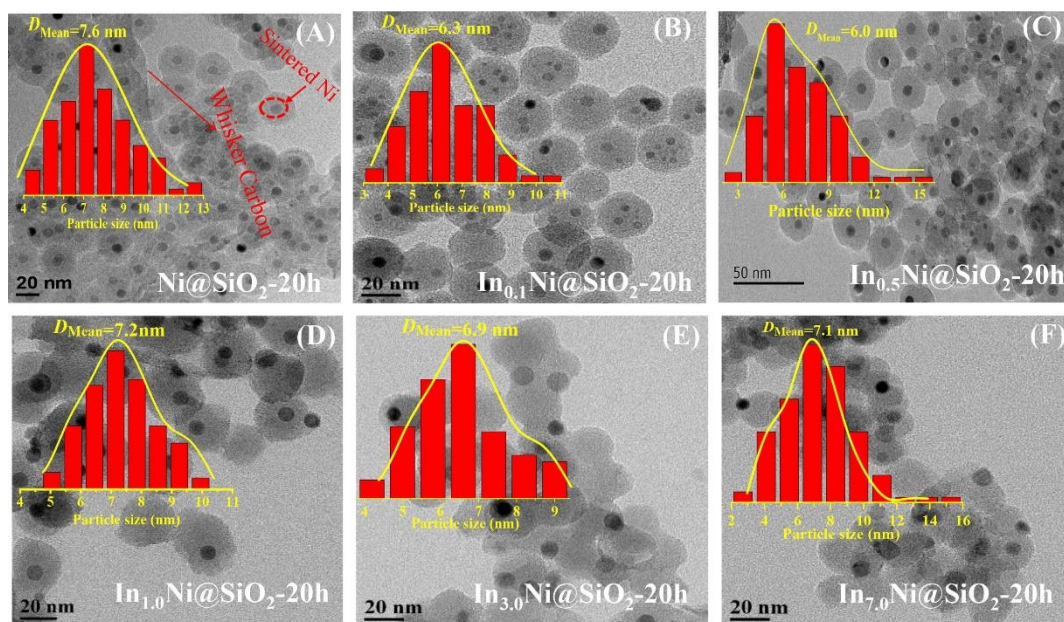


**Figure 8.** TEM images and Ni particle size distributions of spent (A)  $\text{Ni@SiO}_2$ -20 h, (B)  $\text{In}_{0.1}\text{Ni@SiO}_2$  20 h, (C)  $\text{In}_{0.5}\text{Ni@SiO}_2$ -20 h, (D)  $\text{In}_{1.0}\text{Ni@SiO}_2$ -20 h, (E)  $\text{In}_{3.0}\text{Ni@SiO}_2$ -20 h, and (F)  $\text{In}_{7.0}\text{Ni@SiO}_2$ -20 h catalysts. Reprinted with permission from [146]. Copyright (2022) Elsevier.

### 2.3. Noble Metals as Active Phase

The great resistance of noble metals to sintering and coking phenomena makes their applications of high interest in academic and industrial research. Elements such as Pt, Rh and Ru are highly active towards dry reforming and more resistant to carbon deposition than other transition metals [147,148]. Rh-based materials were proposed as effective catalysts for steam reforming [149], dry reforming [147,150], partial oxidation [151] and oxy reforming of methane [152].

In a recent study [153], the coking resistance of Rh 1 wt.% over  $\gamma\text{-Al}_2\text{O}_3$ , Ceria-Zirconia (CZ,  $\text{Ce}_{0.5}\text{Zr}_{0.5}\text{-O}_2\text{-}\delta$ ) and Ceria-Zirconia-Alumina (ACZ, 80 wt.%  $\text{Al}_2\text{O}_3$ -20 wt.%  $\text{Ce}_{0.5}\text{-Zr}_{0.5}\text{-O}_2\text{-}\delta$ ) was assessed. The oxygen storage capacity measured by  $\text{H}_2$ -TPR were 0, 101, 557  $\mu\text{mol O}_2 \text{g}^{-1}$  for  $\gamma\text{-Al}_2\text{O}_3$ , ACZ and CZ, respectively. The catalysts were tested for 12 h of reaction at ambient pressure, 750 °C,  $\text{CH}_4/\text{CO}_2 = 1$  and GHSV of 120,000  $\text{mL h}^{-1}\text{g}^{-1}$ , showing stable performance regardless of the oxide support. Rh/ $\gamma\text{-Al}_2\text{O}_3$  attains the higher activity with a  $\text{CH}_4$  conversion of ~90% in comparison to the lower values of 65–70% exhibited by Rh/CZ and Rh/CZA sample, but an opposite trend was observed when the intrinsic activities of the samples are examined. When the temperature dependence of turnover frequencies (TOFs) is considered, it must be noted that the apparent activation energies for  $\text{CO}_2$  and  $\text{CH}_4$  are reduced, especially for the Rh/CZ catalyst. Moreover, the XPS analyses of the catalysts after exposure to DR clearly show that support composition has an influence on the oxidation state of Rh, demonstrating that the surface oxygen mobility promoted by CZ also contributed to stabilize Rh in its metallic state. The authors also stated that through the formation of a layer of labile  $\text{O}^{2-}$  ions on the Rh surface when supported on oxides with high oxygen mobility, the activation and oxidation of  $\text{CH}_4$  become easier (Figure 9). Since the lifetime of the  $\text{O}^{\delta-}$  species is shortened at high temperature, this

“effective double layer model” is efficient mainly on Rh/CZ catalyst and in the conditions in which low temperature DR is carried out.

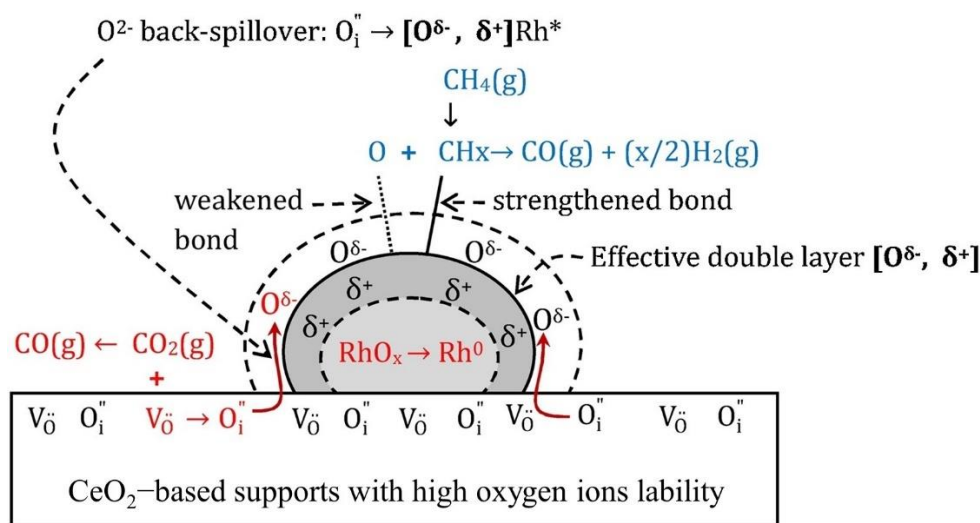


**Figure 9.** Model of the “effective double layer model” in which the dry reforming is promoted by supports with high oxygen ion lability. Reprinted with permission from [153]. Copyright (2019) Elsevier.

The application of Rh/Al<sub>2</sub>O<sub>3</sub> catalyst was also studied by Moral et al. [154], who considered the possibility of adding oxygen to the reaction mixture to perform the catalytic partial oxidation of BG. Under oxy-CO<sub>2</sub> conditions, mainly when a O<sub>2</sub>/CH<sub>4</sub> molar ratio of 0.45 was used, an increase in CH<sub>4</sub> conversion (~85% at 700 °C, GHSV = 150 L<sub>CH<sub>4</sub></sub> g<sub>cat</sub><sup>-1</sup> h<sup>-1</sup>) and H<sub>2</sub> yield (up to ~1.4 mol/mol) was observed, which was not attainable through “classic” dry reforming.

A series of ternary perovskite type BaZr<sub>1-x</sub>Me<sub>x</sub>O<sub>3</sub> containing Rh, Ru or Pt were investigated in the DR of BG by de Caprariis et al. [155]. Unlike Pt perovskite, Rh and Ru catalysts do not show any deactivation with a limited carbon formation rate for BaZrRhO<sub>3</sub> catalyst (0.0019 g<sub>coke</sub> g<sub>cat</sub><sup>-1</sup> h<sup>-1</sup> vs. 0.0027 and 0.0094 g<sub>coke</sub> g<sub>cat</sub><sup>-1</sup> h<sup>-1</sup> for BaZrRuO<sub>3</sub> and BaZrPtO<sub>3</sub>, respectively). The experimental tests point out that the catalyst performance increases following the order Pt < Ru < Rh.

Ru was also found to be an efficient catalyst for dry reforming when supported on Al<sub>2</sub>O<sub>3</sub> [156–158], and MgO [159]. Ru-based catalysts have also been the focus of interesting DFT studies carried out by Egawa [160] and Wang et al. [161], which shed light on CO<sub>2</sub> and CH<sub>4</sub> activation pathways on a Ru (0 0 1) and Ru (0 0 0 1) crystal faces, respectively. The latest work revealed that CO<sub>2</sub> directly dissociates to form O\*, which is the main oxidant of CH<sub>x</sub>\* intermediates. The binding energy difference between these two species increased in the order Ru > Co > Ni > Pd > Pt, which should also reflect the ranking order in terms of resistance to carbon formation. It was found that due to its oxophilic nature, Ru easily activates CO<sub>2</sub>, while CH<sub>4</sub> activation is slower and denoted as the rate-limiting step of reaction, as demonstrated by microkinetic simulations under low-pressure conditions in which the DR reaction rate is clearly affected only by CH<sub>4</sub> pressure.

A Ru-doped Sr<sub>0.9</sub>Y<sub>0.08</sub>TiO<sub>3</sub> perovskite was proposed as highly active in the combined dry reforming and sorption-enhanced WGS process (SE-WGS) for pure H<sub>2</sub> production [162]. The system configuration (Figure 10) involves a first stage in which clean biogas undergoes dry reforming, followed by a second step in which a CuZnAl catalyst (active for WGS) and a CO<sub>2</sub> sorbent (in a ratio of 1:4 wt/wt) are packed in a divided section of a fixed bed reactor that operates at 300 °C. Once the adsorber sites are saturated, the reactor undergoes to a regeneration cycle at 500 °C to desorb CO<sub>2</sub> that can be recycled to DR unit as a reactant.

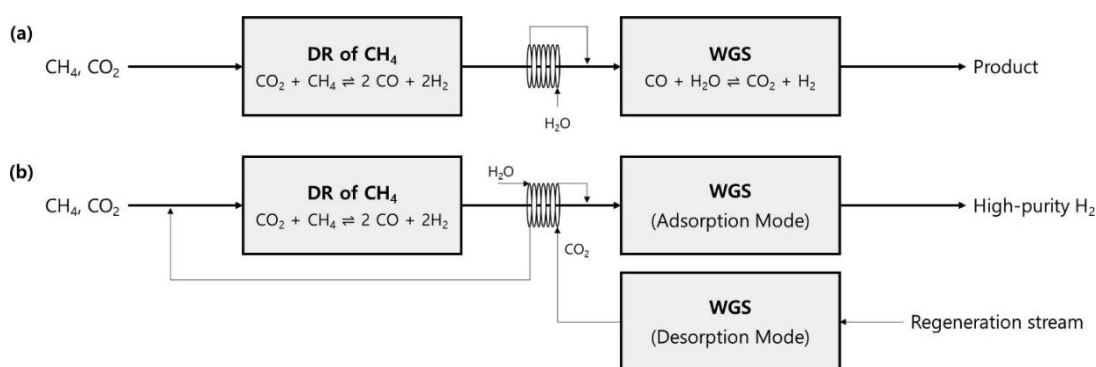


**Figure 10.** Schematic of the integrated systems: (a) combination of DR and WGS reactions and (b) DR and SE-WGS reactions units. Reprinted with permission from [162]. Copyright (2022) Elsevier.

From the XPS analyses conducted on the Ru5-SYT (where 5 is the mol.% of Ru that substitutes Ti in the perovskite structure), it appears that the incorporation of Ru causes a shift to lower binding energy of the peak attributed to the presence of lattice oxygen vacancy (from 529.8 to 529.5 eV). After reduction, Ru formed nanoparticles with an average diameter of 2–4 nm, which were not significantly modified after 100 h of TOS in which the catalyst attains  $\text{CH}_4$  conversion of 82% at 750 °C, GHSV of  $1580 \text{ h}^{-1}$ ,  $\text{CO}_2/\text{CH}_4$  ratio of 1.05. From the results obtained combining the two reactors, it is possible to obtain pure  $\text{H}_2$  (>99.5%) until the saturation of the sorbent, that seems to be the limiting factor of productivities of such units. Nevertheless, the proposed DR/WGS-SE system shows to be resistant to regeneration cycles, which minorly affects the performances of the process.

Pt supported over  $\text{Al}_2\text{O}_3$  and doped  $\text{CeO}_2/\text{Al}_2\text{O}_3$  was studied for the BG reforming by da Fonseca et al. [163]. In this case, the type of promoter and its role on the Pt activity and stability for the dry reforming was studied. The oxygen storage and release capacity of the different catalysts were also studied by in situ XRD and XANES analyses during reduction treatment. It was found that the amount of reduced  $\text{Ce}^{3+}$  sites and the temperature of reduction in  $\text{Ce}^{4+}$  vary among the different Pt/Ce/ $\text{Al}_2\text{O}_3$  samples doped with Pr, Zr and Nb (3–5 wt.%). The Pt/CePr/ $\text{Al}_2\text{O}_3$  catalysts scored the highest  $\text{Ce}^{3+}$  molar fraction (23% vs. 16–17% for the others) and thus reducibility, even if the Pt dispersion value obtained by cyclohexane dehydrogenation was low (9% vs. 42% of Pt/ $\text{Al}_2\text{O}_3$ ). From the catalytic results, it is possible to observe how, after 3 h, the Pt/ $\text{Al}_2\text{O}_3$  catalyst quickly deactivates reaching the lowest BG conversion values (25 and 15% of  $\text{CO}_2$  and  $\text{CH}_4$  conversion, respectively). Instead, the co-presence of Ce and Pr led to a stable performance at 800 °C over 24 h, attaining  $\text{CH}_4$  conversion of 75–72% and  $\text{CO}_2$  conversion of 75–70%. Although the formation of carbon was detected regardless of the catalyst, it was found that the main reason behind deactivation was the sintering of Pt that was detected even in doped samples except for Pt/CePr/ $\text{Al}_2\text{O}_3$ .

#### 2.4. Bimetallic Catalysts

The applications of bimetallic catalysts in BG reforming could be a practical and successful method to overcome catalyst deactivation increasing coke-resistance and mitigating the sintering of the active phase. The Ni stability can be improved by the addition of small amounts of precious metals such as Rh, Ru, Ir, Au, Pd, and Pt or non-precious metals such as Co, Cu, Fe or Sn. Depending on the chemical nature of the two elements, the surface properties of the catalyst change through the formation of alloys, core-shell or nano-sized structures that boost the catalytic performance. The presence of a small amount of Rh in a Ni-Zeolite L catalyst, obtained by incipient wetness impregnation, was found to improve both the dispersion of the active phase and the metal support-interaction to increase the  $\text{H}_2$  production of biogas steam-, oxy- and tri-reforming processes [164]. Ni-Rh catalysts were also found to be highly active and stable in dry reforming or combined steam and dry reforming reaction when supported on  $\text{SiO}_2$  [165],  $\text{CeO}_2\text{-ZrO}_2$  [166], and

$\text{Al}_2\text{O}_3$  [167,168]. In our published work [169] we proposed the use of hydrotalcite-type precursors to obtain Ni-Rh/Mg/Al/O mixed oxides active in dry reforming and steam reforming of biogas. The unique structure of the precursors assured a high dispersion of the metals on the catalyst surface while the formation of a Ni-Rh alloy during reduction avoided the re-oxidation of Ni in the steam reforming conditions. Remarkably, the presence of 0.5 wt.% of Rh suppressed the carbon formation and improved the resistance of the active phase towards sintering and deactivation. Moreover, changing the synthesis method by using a Ni-Rh clusters [72] (deposited on the support via wet impregnation) in which the elements were in intimate contact, it was possible to reduce the amount of Rh and Ni (Figure 11) and simultaneously maintain high activity ( $\text{CH}_4$  and  $\text{CO}_2$  conversions of 92% and 72%, respectively, at 900 °C,  $P = 5$  bar,  $\text{Steam}/\text{CH}_4 = 0.5$ ,  $\text{GHSV} = 50,000 \text{ mL g}_{\text{cat}}^{-1} \text{ h}^{-1}$ ) and stability in the combined steam and dry reforming reaction conditions.

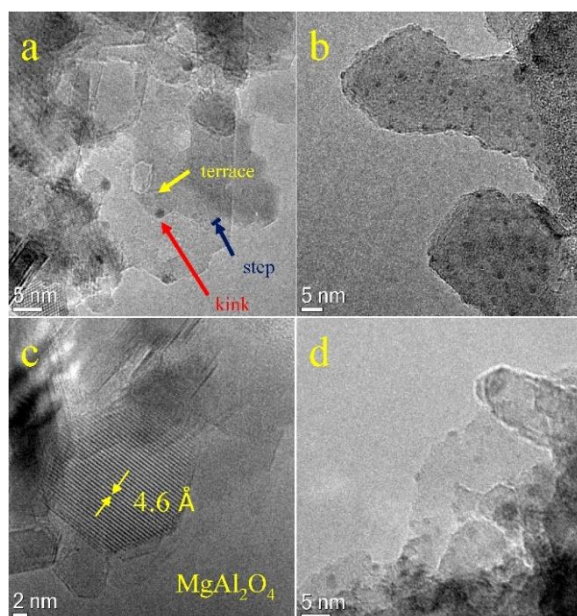


**Figure 11.** HR-TEM images of reduced Ni-Rh/Mg/Al/O catalysts: (a,c,d) Ni 3.0 wt.% Rh 0.5 wt.%; (b) Ni 2.0 wt.% Rh 0.3 wt.% [72].

Since Ni and Ru have a limited miscibility, the Ni-Ru catalysts could be in the form of dispersed mixed particles with a high structural complexity, which need a careful optimization of the synthesis method as an optimal control of structural variations that occur during pre-treatment and catalytic assessments. The combined steam and dry reforming was studied by Alvarez et al. [170] using Ni-Ru catalysts supported on Mg/Al/O. The bimetallic catalysts showed a higher biogas conversion ( $\text{CH}_4$  conversion of 55%,  $\text{CO}_2$  conversion of 50%, at 750 °C with 28% of  $\text{H}_2\text{O}$  in the feed,  $\text{GHSV} 120,000 \text{ mL g}_{\text{cat}}^{-1} \text{ h}^{-1}$ ) if compared to the Ni/Mg/Al/O system and the desired  $\text{H}_2/\text{CO}$  ratio of two in the produced syngas was attained at 750 °C and a  $\text{H}_2\text{O}/\text{CH}_4 = 0.56 \text{ mol/mol}$ . The influence of the metal order addition was investigated performing two impregnation methods. A simultaneous incorporation of the active phase was beneficial in terms of Ni-Ru interactions and Ru dispersion that led to the fast gasification of deposited carbon. The enhanced resistance of this bimetallic systems towards coke deactivation was demonstrated by Zhou et al. [171]. The Ru/Ni/MgO catalysts obtained via solvothermal synthesis of  $\text{Ru}_x\text{Ni}_y\text{Mg}_{1-x-y}(\text{OH})(\text{OCH}_3)$  precursors assured a homogeneous distribution of the elements, especially when this precursor was directly reduced in  $\text{H}_2$  flow at 800 °C, and the amount of incorporated Ru was low. In these conditions, the catalyst attained a high durability of 100 h in the dry reforming at 800 °C, showing  $\text{CH}_4$  and  $\text{CO}_2$  conversions of 95% and 90%, respectively ( $P = 1$  bar,  $\text{GHSV} 86,000 \text{ mL g}_{\text{cat}}^{-1} \text{ h}^{-1}$ ). The authors stated that the formation of a Ru-rich overlayer during reaction conditions had the ability to slow  $\text{CH}_4$  dissociation while enhanc-

ing the surface oxygen coverage and the carbon oxidation by CO<sub>2</sub>. Similar results were reported by Xu et al. [172]; that via combustion method were able to synthesize a series of Ni(Zr,Ru)/SiO<sub>2</sub> catalysts with an improved Ni dispersion hardly attainable with conventional impregnation technique. The small particles size (~5 nm), together with the strong metal-support interactions brought by the fast synthesis method, assured high catalytic activity while the presence of carbonaceous deposits after 50 h of reaction decreased in the order Ni/SiO<sub>2</sub> > NiZrO<sub>2</sub>/SiO<sub>2</sub> > Ni-Ru/SiO<sub>2</sub>.

Ni-Pd and Ni-Pt catalysts were investigated in both steam and dry reforming of BG. Batebi et al. [173] developed a Ni-Pd/Al<sub>2</sub>O<sub>3</sub> catalyst synthesized via sol-gel method for the combined steam and dry reforming reaction. From the H<sub>2</sub>-TPR results they observed that the synergic interaction between the two metals enhanced the reduction degree of NiO, leading to better dispersed nanoparticles that highly improved the CH<sub>4</sub> conversion and the H<sub>2</sub> yield of the reaction. Similar results were obtained in the DR by Pan and co-workers [174] that tested a series of Ni-Pd/SiO<sub>2</sub> catalysts obtained via oleic acid-assisted wet impregnation method. The results demonstrates that the size of the formed Ni-Pd nanoparticles do not change during reaction, highlighting their superior resistance towards sintering phenomena. The catalyst attained good stability over 1500 min of TOS and a CH<sub>4</sub> conversion of 65% at 700 °C, higher than that of monometallic catalyst (CH<sub>4</sub> conversion of 50%). Similarly, a Ni-Pt/Al<sub>2</sub>O<sub>3</sub> [175] catalyst was found to be highly active in dry and combined steam/dry reforming in the 600–800 °C temperature range. In addition to changing the reduction properties of the catalyst, the presence of Pt highly decreases the carbon deposition. Li et al. [176] studied the evolution of surface composition of a series Ni-Pt/Al<sub>2</sub>O<sub>3</sub> catalysts under simulated reaction conditions. The results obtained using various techniques such as XANES, XPS, HAADF-STEM demonstrate that upon thermal treatment, the active phase undergoes a surface reconstruction in which Pt monolayer island-modified Ni nanoparticles obtained during synthesis evolve to core-shell bimetallic sites composed of a Ni-rich center. As the Pt coverage increases, the activity is enhanced through a facilitation of the CH oxidation pathway, which contributes to the suppression of carbon deposition.

The formation of a Ni-Co alloy can boost the catalytic performance and increase the stability of the catalyst. As demonstrated by HAADF-STEM and EXAFS experiments, the formation of this active phase took place beyond 600 °C [177]. An optimal Ni/Co ratio over  $\gamma$ -Al<sub>2</sub>O<sub>3</sub>/La<sub>2</sub>O<sub>3</sub> could improve pore textural properties and enhance metal particle dispersion that led to stable performance over 290 h in dry reforming reaction (CH<sub>4</sub> and CO<sub>2</sub> conversion equal to 94%, GHSV 6000 mL g<sub>cat</sub><sup>-1</sup> h<sup>-1</sup>, T = 800 °C) [178]. Moreover, the oxygen affinity of Co increases the carbon oxidation rate, while hydrogen spillover from Ni to Co prevents its oxidation in the reforming conditions [101]. In this sense, a Ni-Co/Al/Mg/O obtained by coprecipitation showed impressive stability for 250 h at 750 °C, GHSV of 110,000 mL g<sub>cat</sub><sup>-1</sup> h<sup>-1</sup> with very low carbon formation when Ni and Co concentrations were low (3.6 and 4.9 mol.% respectively) [179]. More recently, Fan and co-workers [180] demonstrated the improved stability of a Ni-Co/MgO nanoplate solid solution, which after reaction formed small Ni-Co alloyed nanoparticles (d ~5 nm) that were active in dry reforming for 1000 h of TOS. The mechanism behind the Ni-Co particles formation and evolution in DR was studied by in situ scanning transmission X-ray Microscopy by Askari et al. [181] under reducing and operating conditions. Interestingly, when in calcined form, the Ni-Co/ $\gamma$ -Al<sub>2</sub>O<sub>3</sub> catalyst exhibited an inhomogeneous distribution of Ni and Co. A reduction in this system led to elemental segregation that involved Co migration to the center of the forming nanoparticles while Ni occupied the outer shell of the bimetallic phase. It turned out that this structure was preserved during reaction, creating a synergic site in which Ni acted as main active phase whereas Co serves as electron donor to boost activity and carbon gasification.

Among the transition metals series, Fe was also found to enhance Ni catalysis in biogas reforming processes. As demonstrated by Theofanidis et al. [182], depending on the Ni/Fe ratio, it is possible to obtain a catalyst with good activity in dry reforming using MgAl<sub>2</sub>O<sub>4</sub>

as support ( $STY = 0.110 \text{ mol}_{\text{CH}_4} \text{ s}^{-1} \text{ mol}_{\text{Ni}}^{-1}$  at  $750 \text{ }^\circ\text{C}$ ). Moreover, the structural evolution of the bimetallic particles under reducing and oxidizing conditions was monitored using time-resolved in situ X-ray diffraction. The formation of the Ni-Fe alloy was found to occur beyond  $500 \text{ }^\circ\text{C}$ . However, the bimetallic phase underwent decomposition in the presence of  $\text{CO}_2$  after  $600 \text{ }^\circ\text{C}$  to form Ni and  $\text{Fe}_3\text{O}_4$ . In accordance with their new findings [183], this peculiar behavior is beneficial during biogas reforming as, depending on  $\text{CH}_4/\text{CO}_2$  ratio, the alloy can be partially decomposed through Fe segregation (Figure 12). The Fe-oxide decorates the alloyed nanoparticles, reducing carbon accumulation at its surface by a fast interaction with  $\text{FeO}_x$  lattice oxygen, that produced CO.

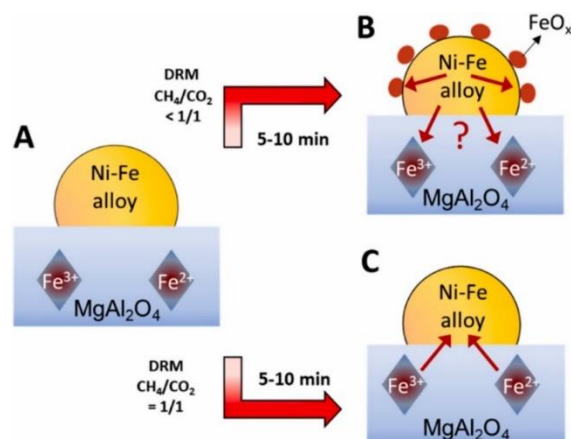


**Figure 12.** Schematic representation of the compositional changes in: (A) reduced NiFe/MgAl<sub>2</sub>O<sub>4</sub> catalyst, (B) during DR with  $\text{CH}_4/\text{CO}_2 < 1$ , and (C) during DR with  $\text{CH}_4/\text{CO}_2 = 1$ , as suggested by in situ QXAS. Red arrows in B and C indicate Fe mobility. Reprinted with permission from [183]. Copyright (2022) Elsevier.

### 2.5. Structured Catalysts

Structured catalysts enhance mass and heat transfer rates and decrease pressure drop, thus being an optimum choice to decrease temperature gradients in the reforming of biogas and working at high GHSV under transient conditions [184]. Hence, small scale reactors operating under transient conditions can be developed. Ni and/or noble metal-based catalysts coated on several structured supports, such as honeycomb monoliths or open-cell foams, have been proposed for the biogas reforming, also in presence of  $\text{O}_2$  and  $\text{H}_2\text{O}$ .

A Ni catalyst promoted with small amounts of Ru coated on honeycomb cordierite monoliths displays an enhanced activity in the reforming of biogas in comparison to a packed bed reactor (85% of  $\text{CO}_2$  conversion vs. 45%). However, the real effect of the structured support is not clear, since the enhancement in the activity is related to differences in the contact time, the latter is larger over the monolith than the packed bed [185]. The interaction of the catalytic coating with the cordierite support, which depends on the calcination time, modifies the catalytic phases in a Ni/ $\gamma$ -Al<sub>2</sub>O<sub>3</sub> washcoated cordierite monolith due to the formation of a Ni<sub>1-x</sub>Mg<sub>x</sub>Al<sub>2</sub>O<sub>4</sub> spinel [186]. The diffusion of Mg from the cordierite monolith to the catalyst coating during calcination at  $800 \text{ }^\circ\text{C}$  for 20 h leads to the formation of a higher amount of Ni<sub>1-x</sub>Mg<sub>x</sub>Al<sub>2</sub>O<sub>4</sub> than when it is calcined for 4 and 10 h, which produces smaller Ni<sup>0</sup> particles and decreases the carbon deposition in the reforming of biogas. A nanocomposite Ni + Ru/Ce<sub>0.35</sub>Zr<sub>0.35</sub>Pr<sub>0.3</sub>O<sub>2</sub>/mesoporous MgAl<sub>2</sub>O<sub>4</sub> loaded on a honeycomb FeCralloy foil substrate shows a high performance and stability to coking in the autothermal natural gas oxy-dry reforming with real concentrated feeds [187].

The conventional preparation method of structured catalysts is the washcoating of ready-made catalysts [188]. However, some alternative methods have been also described, and some of them applied to prepare honeycomb-based biogas reforming catalysts. Cordierite monoliths (400 cpsi) coated with Ni, Rh, or Pt on CeO<sub>2</sub> are prepared by a combination of solution combustion synthesis and wetness impregnation (Figure 13) [189].



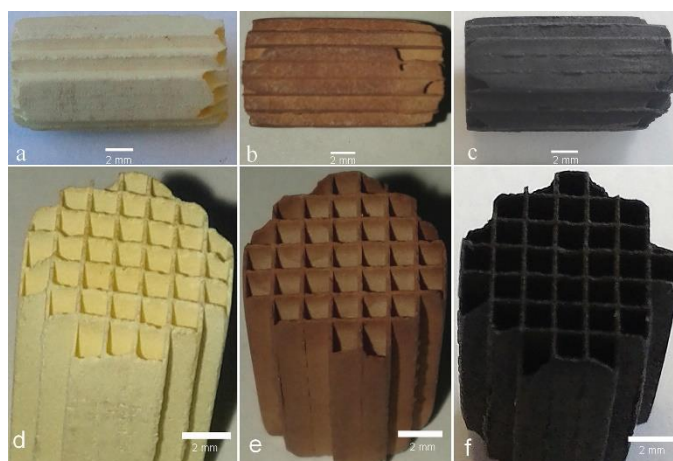


**Figure 13.** Structured systems after  $\text{CeO}_2$  deposition by solid combustion synthesis and calcination at  $600\text{ }^\circ\text{C}$  (a,d), after Rh impregnation by wetness impregnation (b,e) and after the final calcination at  $400\text{ }^\circ\text{C}$  (c,f). Reprinted with permission from [189]. Copyright (2018) Elsevier.

Thin and evenly coated layers with high mechanical strength are obtained, and for Rh/ $\text{CeO}_2$  a stable activity for 200 h in the steam ( $S/C = 3$ ) and oxygen steam reforming ( $S/C = 1$ ,  $O/C = 0.2$ ) of biogas is obtained at  $900\text{ }^\circ\text{C}$  and  $180,000\text{ NmL g}_{\text{cat}}^{-1}\text{ h}^{-1}$  ( $\text{CH}_4$  conversion of 95–100%,  $\text{H}_2/\text{CO}$  ratio of the outlet stream  $\sim 3\text{ mol/mol}$ ). Akri et al. prepared bulk monoliths; a catalyst, based on natural illite clay, nickel, and magnesium, is added into moldable paste easily extruded into a honeycomb monolith [29].

The shape of the structured support may also determine the catalytic properties. By comparing the performance in the steam and oxygen biogas reforming at  $700\text{--}800\text{ }^\circ\text{C}$  and  $250,000\text{--}350,000\text{ NmL g}_{\text{cat}}^{-1}\text{ h}^{-1}$  of Ni/ $\text{CeO}_2$  and Ni-Rh/ $\text{CeO}_2$  catalysts coated on cordierite honeycomb monoliths (500 cpsi) and  $\text{Al}_2\text{O}_3$  (30 ppi) open-cell foams, it is shown that the foams provide better results due to more efficient heat and mass transfer phenomena, attributed to the random porous network of foam support [190]. The effect of the promotion of Rh is also evidenced; NiRh-based catalysts perform better than Ni-based systems, mainly under less favored reaction conditions, i.e., low temperatures and high space velocity.

The dimensions of pores per inch (ppi) in the foams modify the catalytic properties in the steam reforming of biogas with steam and oxygen [191]. Over Rh/ $\text{CeO}_2$  on  $\text{Al}_2\text{O}_3$  foams the activity follows the order  $20 < 30 \sim 40\text{ ppi}$  at high spatial velocities ( $35,000\text{--}140,000\text{ NmL g}^{-1}\text{ h}^{-1}$ ). External interphase (gas-solid) and external diffusion are improved by reducing the pore diameter of the open-cell foams. The best catalyst shows a stable activity for both steam ( $\text{CH}_4$  and  $\text{CO}_2$  conversions of 100% and 14%, respectively) and oxy-reforming ( $\text{CH}_4$  conversion of 100%,  $\text{CO}_2$  conversion of 50%) at  $T_{\text{SET}} = 900\text{ }^\circ\text{C}$  and  $70,000\text{ NmL g}^{-1}\text{ h}^{-1}$  for 200 h of time-on-stream with consecutive start-up and shut-down cycles.

Structured supports made of heat conductive materials are preferred to enhance the heat transfer. In this sense, Ni- $\text{CeO}_2$ - $\text{Al}_2\text{O}_3$  supported on SiC foams have been used in the reforming of biogas [192]. The enhanced activity of the catalyst in the reforming of biogas is related to the in situ development of  $\text{CeAlO}_3$ , able to activate  $\text{CO}_2$ , and uniformly distributed Ni nanoparticles. Liquid silicon-infiltrated SiC (Si-SiC) foams, to avoid the oxidation of SiC, are coated with a 10–0.3 wt.% Ni–Rh/ $\text{MgAl}_2\text{O}_4$  catalyst and studied for the autothermal reforming of model biogas for the production of fuel cell hydrogen [193]. The heat conductivity of the support, however, does not allow the reactor to be operated at isothermal conditions, due to the succession of fast strongly exothermic and endothermic reactions. Structured catalysts based on SiC (Figure 14) have also been applied in the autothermal reforming of biogas coupled to a catalytic wall-flow filter to retain soot particles [194].

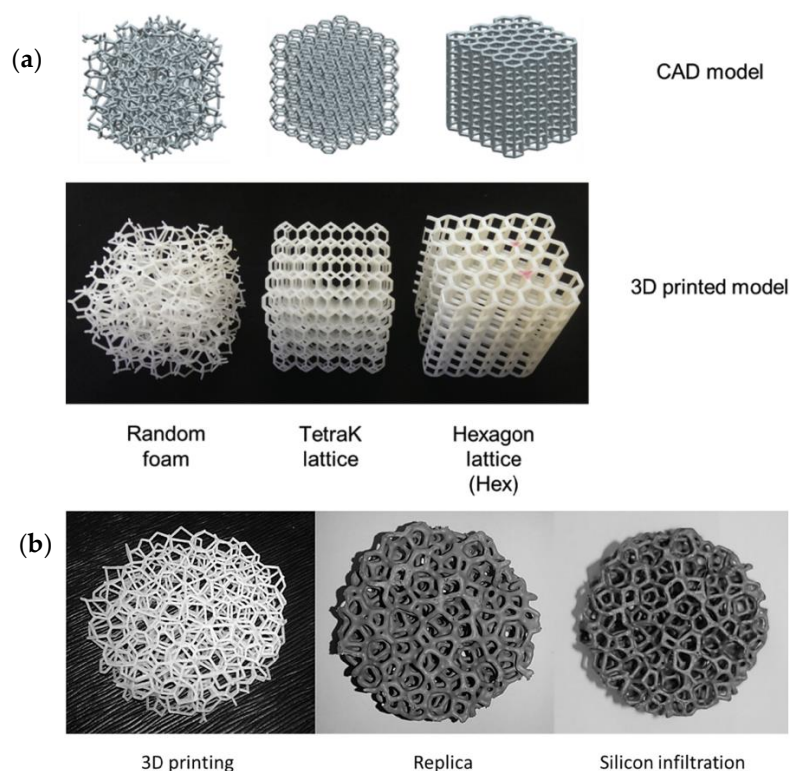


**Figure 14.** (a) Regular and random structures designed and printed; (b) the processing phases of a porous SiSiC body. Reprinted with permission from [194]. Copyright (2018) Elsevier.

Homogenous lattices made by Cubic, Octet and Kelvin cells and the conventional open-cell foam supports, designed by modelling [195], are manufactured by replica of 3D-printed structures followed by Silicon infiltration. After coating, a 15–0.05 wt.-%-Ni-Rh/MgAl<sub>2</sub>O<sub>4</sub>-SiSiC structured catalyst is evaluated in a lab bench, a pilot test rig, and a demonstration plant. The pre-commercial processor is reliable, showing a negligible pressure drop.

Metal foams also show a higher thermal conductivity than ceramic foams. A Ni foam is used to enhance the radial heat transfer of a reactor for the combined steam and dry reforming of methane in the gas to liquid-floating production storage and offloading process [196]. An optimized Ni/ $\gamma$ -Al<sub>2</sub>O<sub>3</sub>/Ni foam, with a highly adherent coating, leads to a uniform temperature distribution along the catalyst-bed operating at high space velocity values, and in turn allows the process intensification. Moreover, a NiCrAl metal-foam coated by a 0.09 wt.-% [Pd(7)–Rh(1)]/(CeZrO<sub>2</sub>–Al<sub>2</sub>O<sub>3</sub>) catalyst performs better than commercially available alumina-supported 8.0 wt.-% Ru and 13.0 wt.-% Ni catalysts in the steam reforming of a model biogas (60% CH<sub>4</sub> and 40% CO<sub>2</sub>) at 10.13 bar. The experimental activity of this catalyst in a heat reactor platform is compared with simulated data [197]; experimental CH<sub>4</sub> conversion is close to that of the equilibrium at 700 °C for CH<sub>4</sub>/CO<sub>2</sub> = 60/40 and S/C = 1.5 and above, whereas experimental CO<sub>2</sub> conversion does not reach the equilibrium values within the temperature range tested. The authors state that the biogas reformer coupled with a Solid Oxide Fuel Cell can provide a viable approach to exploit distributed renewable methane resources for delocalized power generation. We have recently reported the coating of NiCrAl foams by Ru or Rh/Mg/Al hydrotalcite-type compounds through electrodeposition [198]. After calcination, a thin and stable film of oxides is obtained, which after reduction contains Rh or Ru nanoparticles highly dispersed and stabilized by a strong metal support interaction. Moreover, the coating comprises Ni particles segregated from the foam under reduction and reaction conditions. Rh-based catalysts show superior activity (CH<sub>4</sub>, CO<sub>2</sub> conversion of 88% and 48%, respectively at 900 °C, S/CH<sub>4</sub> = 1, GHSV = 40,000 h<sup>-1</sup>) and stability with the time on stream than Ru

catalyst. The structured catalysts allowed them to operate at higher space velocities and low Steam to CH<sub>4</sub> ratio, than a pelletized catalyst, increasing the biogas valorization and thus the productivity (Figure 15).

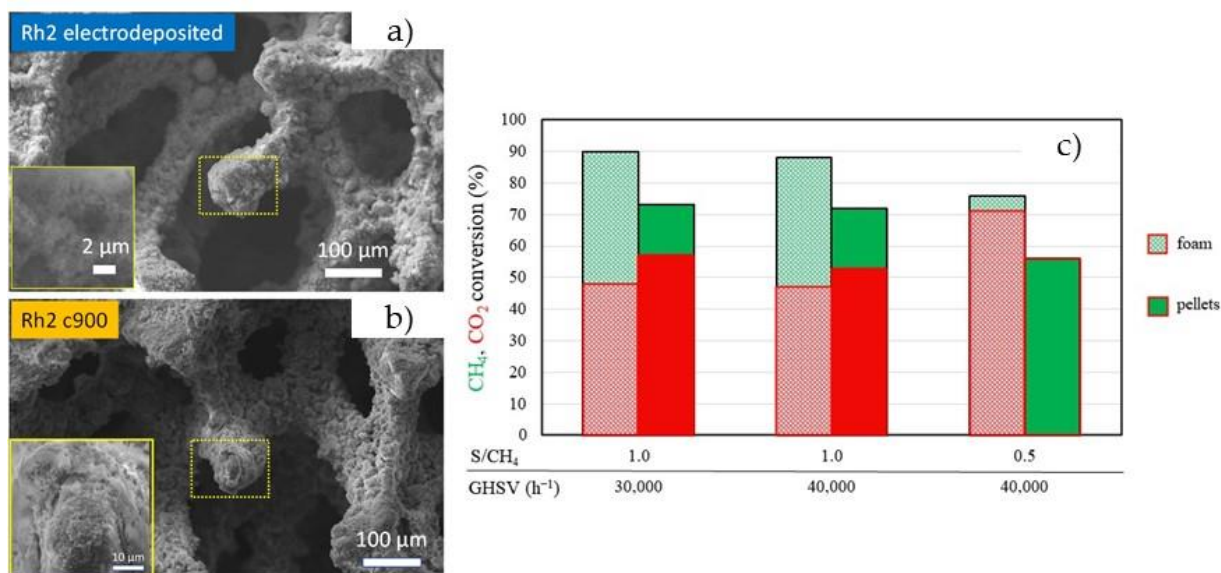


**Figure 15.** (a) SEM images of Rh2/Mg/Al/O precursor; (b) SEM images of Rh2/Mg/Al/O after calcination at 900 °C and (c) Comparison of CH<sub>4</sub> and CO<sub>2</sub> conversion values of a pelletized catalyst and Rh5/Mg/Al/O structured catalyst. The Rh loading in the reactor is kept constant for both pelletized and structured beds, T = 900 °C, P = 5 bar. Reprinted with permission from [198]. Copyright (2022) Elsevier.

Lastly, paper structured catalysts (fibers, Figure 16) containing Ni loaded on CeO<sub>2</sub> flowers [199] and (Ce,Zr)O<sub>2-δ</sub> [200] are also investigated in the reforming of biogas. The enhanced activity is related to the small Ni particles and the oxygen storage capacity of the ceramic supports rather to the structuration of the catalysts.

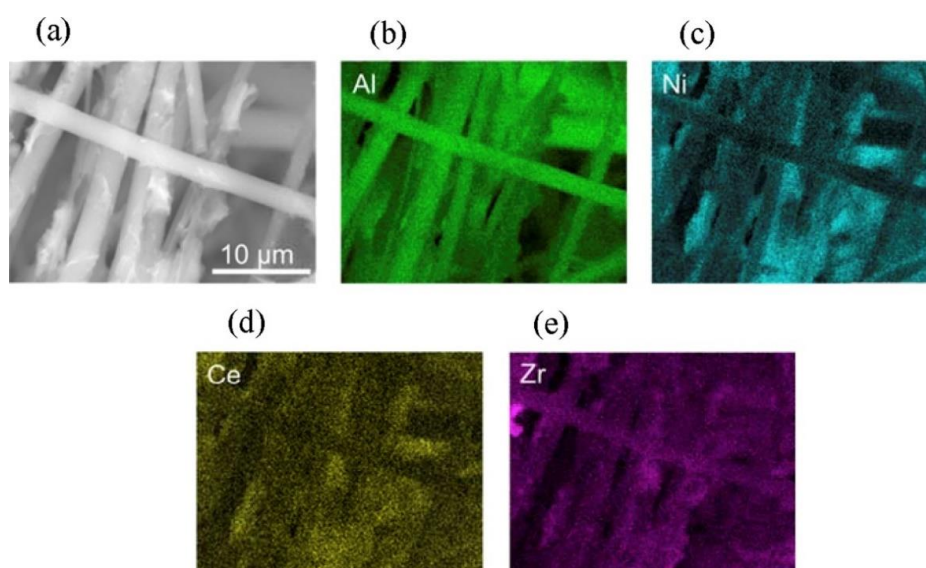


**Figure 16.** Images of a paper structured catalyst after reduction treatment at 750 °C in 5% H<sub>2</sub> for 5 h; (a) FE-SEM image and corresponding EDX mapping images of (b) Al, (c) Ni, (d) Ce and (e) Zr. Reprinted with permission from [200]. Copyright (2018) Elsevier.

### 3. Conclusions and Perspectives

Biogas upgrading through reforming reactions is a promising technology that allows a syngas to be obtained that can be further converted into products with high added value such as hydrogen, synthetic fuels, methanol, dimethyl ether, etc. Depending on the process, the catalyst should cope with several issues related to the harsh reaction conditions used and the need for long-term stability, essential for developing solid industrial technologies.

The severe carbon formation that may take place during biogas dry reforming is the main obstacle to the industrialization of this process. Adding water or oxygen to the inlet stream to perform combined reforming can help to deal with this issue, but the sintering of the active phase or its reoxidation could easily occur, mining the catalyst activity and stability. In this sense, the accurate choice of the active phase and catalytic support plays a fundamental role in obtaining high and stable catalytic performances. The use of promoters or supports with high oxygen mobility/storage (such as CeO<sub>2</sub>, CeO<sub>2</sub>/ZrO<sub>2</sub> and in some extent La<sub>2</sub>O<sub>3</sub>) may enhance carbon gasification rate, reducing the deposition of the carbonaceous materials. Other promoters (MnO, Fe/O) can block the catalytic sites responsible for carbon polymerization, avoiding the formation of filamentous carbon while the use of elements able to modify the redox properties of the catalyst (such as Rh, Pd, In<sub>2</sub>O<sub>3</sub>, CeO<sub>2</sub>, Fe/O, ZnO) increases the tendency to adsorb and activate CO<sub>2</sub> and CH<sub>4</sub>. Moreover, the establishment of strong metal support interactions by using various catalyst preparation techniques can improve the active metal distribution and stability, avoiding the sintering phenomena that can occur at the high temperatures of reaction.

The use of a noble metal (such as Rh, Pt and Ru) as active phase can enhance the catalyst performance, but at the expense of a higher cost that, depending on the catalyst design, may be not economically viable (especially in the case of Rh-based catalysts). In this sense, the use of a bimetallic catalyst could be an appropriate choice to decrease the production costs and obtain high reaction rates. In this context, the formation of alloys (Ni-Rh, Ni-Co, Ni-In, Ni-Zn, Ni-Fe) and nanostructured reaction sites (Ni-Ru, Ni-Pt), boost the catalyst activity through synergistic effects that increase the dispersion of the active phase and its resistance towards deactivation.

Finally, the proper structurization of the reforming catalyst and reactor, by using ceramic or metallic supports, can improve the process productivity, assuring high mass and heat transfer, as well as minimizing the amount of catalyst loaded.

As it was possible to observe from the review of recent publications, the research on biogas reforming will probably be even more focused on a deeper understanding of reaction mechanisms and on the phenomena that lead to catalyst deactivation. The extensive use of advanced operando techniques such as EXAFS, XANES, XPS and FTIR spectroscopy can greatly help to shed light on the key reaction pathways, intermediates, and surface evolution that occur during the catalytic process.

The use of innovative synthesis methods able to address specific nano structurization of the active sites (core shell sites, alloyed active phases and Yolk-shell catalysts), could greatly improve the catalysts resistance towards sintering and coking and in turn their activity and stability in the reforming reactions.

Although the use of monometallic Ni-based catalysts leads to economic advantages, it has been widely proven that the use of these systems has many limitations related to the lack of resistance towards carbon deposition, especially in the dry reforming. In this context, the near future research should be focused on the further improvement of Ni-bimetallic catalysts, aiming to maximize their economic viability by lowering the loading of the noble metal or by using cheaper promoters such as Fe, Zn and Co. In this sense, an optimum combination of a highly active metallic center and support with improved oxygen mobility would assure both great performance and catalyst lifetime.

The great potential of structured catalysts as possible systems to improve heat and mass transfer, and increase the plant productivity, could be the turning point to further develop processes able to operate at a lower temperature without massive carbon formation. To do so, an accurate engineering of the reactor design, together with the optimization

of the catalyst resistance in industrial conditions, are of paramount importance for the scale-up of the process.

Particular attention should be focused on catalytic assessments that simulate real industrial conditions that comprise also the use of high pressures that, although increase carbon formation, can drastically decrease operational costs that would certainly accelerate the industrialization of biogas reforming technologies.

**Author Contributions:** N.S., M.B., C.L., P.B. and A.G.D.G. collected some part of the literature and wrote the respective part. A.V. and G.F. supervised and revised the work. All authors have read and agreed to the published version of the manuscript.

**Funding:** This research received no external funding.

**Institutional Review Board Statement:** Not applicable.

**Informed Consent Statement:** Not applicable.

**Data Availability Statement:** Not applicable.

**Conflicts of Interest:** The authors declare no conflict of interest.

## References

1. The Paris Agreement | UNFCCC. Available online: <https://unfccc.int/process-and-meetings/the-paris-agreement/the-paris-agreement> (accessed on 9 December 2021).
2. What Is a COP? Available online: <https://ukcop26.org/uk-presidency/what-is-a-cop/> (accessed on 12 December 2021).
3. Glasgow Climate Change Conference—October–November 2021 | UNFCCC. Available online: <https://unfccc.int/conference/glasgow-climate-change-conference-october-november-2021> (accessed on 12 December 2021).
4. US EPA. Understanding Global Warming Potentials. Available online: <https://www.epa.gov/ghgemissions/understanding-global-warming-potentials> (accessed on 12 December 2021).
5. CO<sub>2</sub> and Greenhouse Gas Emissions—Our World in Data. Available online: <https://ourworldindata.org/co2-and-other-greenhouse-gas-emissions> (accessed on 12 December 2021).
6. Methane: A Crucial Opportunity in the Climate Fight. Available online: <https://www.edf.org/climate/methane-crucial-opportunity-climate-fight> (accessed on 12 December 2021).
7. World Resources Institute. *STATEMENT: Bright Spots at COP26 Need to Turn into Action and Even More Ambition in 2022*; World Resources Institute: Washington, DC, USA, 2021.
8. Joint EU-US Press Release on the Global Methane Pledge. Available online: [https://ec.europa.eu/commission/presscorner/detail/en/IP\\_21\\_4785](https://ec.europa.eu/commission/presscorner/detail/en/IP_21_4785) (accessed on 12 December 2021).
9. Homepage | Global Methane Pledge. Available online: <https://www.globalmethanepledge.org/> (accessed on 12 December 2021).
10. US EPA. Inventory of U.S. Greenhouse Gas Emissions and Sinks: 1990–2019. Available online: <https://www.epa.gov/ghgemissions/inventory-us-greenhouse-gas-emissions-and-sinks-1990-2019> (accessed on 12 December 2021).
11. World Biogas Association. *Biogas: Pathways to 2030—Report*; World Biogas Association: London, UK, 2021.
12. Biogas. Available online: <https://bioenergyeurope.org/article/309-biogas.html> (accessed on 12 December 2021).
13. Andriani, D.; Wresta, A.; Atmaja, T.D.; Saepudin, A. A Review on Optimization Production and Upgrading Biogas Through CO<sub>2</sub> Removal Using Various Techniques. *Appl. Biochem. Biotechnol.* **2014**, *172*, 1909–1928. [CrossRef] [PubMed]
14. Biogas Production: Current State and Perspectives | SpringerLink. Available online: <https://link.springer.com/article/10.1007/s00253-009-2246-7> (accessed on 12 December 2021).
15. Kapoor, R.; Ghosh, P.; Tyagi, B.; Vijay, V.K.; Vijay, V.; Thakur, I.S.; Kamyab, H.; Nguyen, D.D.; Kumar, A. Advances in Biogas Valorization and Utilization Systems: A Comprehensive Review. *J. Clean. Prod.* **2020**, *273*, 123052. [CrossRef]
16. Outlook for Biogas and Biomethane: Prospects for Organic Growth—Analysis—IEA. Available online: <https://www.iea.org/reports/outlook-for-biogas-and-biomethane-prospects-for-organic-growth> (accessed on 12 December 2021).
17. Biogas Trends for This Year | European Biogas Association. Available online: <https://www.europeanbiogas.eu/biogas-trends-for-this-year/> (accessed on 12 December 2021).
18. US EPA. What Is CHP? Available online: <https://www.epa.gov/chp/what-chp> (accessed on 12 December 2021).
19. Sun, Q.; Li, H.; Yan, J.; Liu, L.; Yu, Z.; Yu, X. Selection of Appropriate Biogas Upgrading Technology—a Review of Biogas Cleaning, Upgrading and Utilisation. *Renew. Sustain. Energy Rev.* **2015**, *51*, 521–532. [CrossRef]
20. Jin, Y.; Chen, T.; Chen, X.; Yu, Z. Life-Cycle Assessment of Energy Consumption and Environmental Impact of an Integrated Food Waste-Based Biogas Plant. *Appl. Energy* **2015**, *151*, 227–236. [CrossRef]
21. Collet, P.; Hélias, A.; Lardon, L.; Ras, M.; Goy, R.-A.; Steyer, J.-P. Life-Cycle Assessment of Microalgae Culture Coupled to Biogas Production. *Bioresour. Technol.* **2011**, *102*, 207–214. [CrossRef]
22. Yu, Q.; Li, H.; Deng, Z.; Liao, X.; Liu, S.; Liu, J. Comparative Assessment on Two Full-Scale Food Waste Treatment Plants with Different Anaerobic Digestion Processes. *J. Clean. Prod.* **2020**, *263*, 121625. [CrossRef]

23. Rajabi Hamedani, S.; Villarini, M.; Colantoni, A.; Carlini, M.; Cecchini, M.; Santoro, F.; Pantaleo, A. Environmental and Economic Analysis of an Anaerobic Co-Digestion Power Plant Integrated with a Compost Plant. *Energies* **2020**, *13*, 2724. [CrossRef]
24. Whiting, A.; Azapagic, A. Life Cycle Environmental Impacts of Generating Electricity and Heat from Biogas Produced by Anaerobic Digestion. *Energy* **2014**, *70*, 181–193. [CrossRef]
25. Goulding, D.; Power, N. Which Is the Preferable Biogas Utilisation Technology for Anaerobic Digestion of Agricultural Crops in Ireland: Biogas to CHP or Biomethane as a Transport Fuel? *Renew. Energy* **2013**, *53*, 121–131. [CrossRef]
26. Murphy, J.D.; McKeogh, E. Technical, Economic and Environmental Analysis of Energy Production from Municipal Solid Waste. *Renew. Energy* **2004**, *29*, 1043–1057. [CrossRef]
27. Edwards, J.; Othman, M.; Burn, S.; Crossin, E. Energy and Time Modelling of Kerbside Waste Collection: Changes Incurred When Adding Source Separated Food Waste. *Waste Manag.* **2016**, *56*, 454–465. [CrossRef]
28. Monthly and Annual Prices of Road Fuels and Petroleum Products. Available online: <https://www.gov.uk/government/statistical-data-sets/oil-and-petroleum-products-monthly-statistics> (accessed on 12 December 2021).
29. Akri, M.; Achak, O.; Granger, P.; Wang, S.; Batiot-Dupeyrat, C.; Chafik, T. Autothermal Reforming of Model Purified Biogas Using an Extruded Honeycomb Monolith: A New Catalyst Based on Nickel Incorporated Illite Clay Promoted with MgO. *J. Clean. Prod.* **2018**, *171*, 377–389. [CrossRef]
30. Baena-Moreno, F.M.; Sebastia-Saez, D.; Pastor-Pérez, L.; Reina, T.R. Analysis of the Potential for Biogas Upgrading to Syngas via Catalytic Reforming in the United Kingdom. *Renew. Sustain. Energy Rev.* **2021**, *144*, 110939. [CrossRef]
31. Ardolino, F.; Arena, U. Biowaste-to-Biomethane: An LCA study on biogas and syngas roads. *Waste Manage.* **2019**, *87*, 441–453. [CrossRef] [PubMed]
32. Tajima, H.; Yamasaki, A.; Kiyono, F. Energy Consumption Estimation for Greenhouse Gas Separation Processes by Clathrate Hydrate Formation. *Energy* **2004**, *29*, 1713–1729. [CrossRef]
33. Bekkering, J.; Broekhuis, A.A.; van Gemert, W.J.T. Optimisation of a Green Gas Supply Chain—A Review. *Bioresour. Technol.* **2010**, *101*, 450–456. [CrossRef] [PubMed]
34. Basu, S.; Khan, A.L.; Cano-Odena, A.; Liu, C.; Vankelecom, I.F.J. Membrane-Based Technologies for Biogas Separations. *Chem. Soc. Rev.* **2010**, *39*, 750–768. [CrossRef]
35. Gupta, M.; Coyle, I.; Thambimuthu, K. CO<sub>2</sub> Capture Technologies and Opportunities in Canada: Strawman Document for CO<sub>2</sub> Capture and Storage (CC&S) Technology Roadmap. In Proceedings of the 1st Canadian CC&S Technology Roadmap Workshop, Calgary, AB, Canada, 18–19 September 2003.
36. Adelt, M.; Wolf, D.; Vogel, A. LCA of Biomethane. *J. Nat. Gas Sci. Eng.* **2011**, *3*, 646–650. [CrossRef]
37. Natividad Pérez-Camacho, M.; Curry, R.; Cromie, T. Life Cycle Environmental Impacts of Biogas Production and Utilisation Substituting for Grid Electricity, Natural Gas Grid and Transport Fuels. *Waste Manag.* **2019**, *95*, 90–101. [CrossRef]
38. Lyng, K.-A.; Brekke, A. Environmental Life Cycle Assessment of Biogas as a Fuel for Transport Compared with Alternative Fuels. *Energies* **2019**, *12*, 532. [CrossRef]
39. Cucchiella, F.; D’Adamo, I.; Gastaldi, M. Profitability Analysis for Biomethane: A Strategic Role in the Italian Transport Sector. *Int. J. Energy Econ. Policy* **2015**, *5*, 440–449.
40. Chen, Q.; Wang, D.; Gu, Y.; Yang, S.; Tang, Z.; Sun, Y.; Wu, Q. Techno-Economic Evaluation of CO<sub>2</sub>-Rich Natural Gas Dry Reforming for Linear Alpha Olefins Production. *Energy Convers. Manag.* **2020**, *205*, 112348. [CrossRef]
41. Ahmadi Moghaddam, E.; Ahlgren, S.; Hultberg, C.; Nordberg, Å. Energy Balance and Global Warming Potential of Biogas-Based Fuels from a Life Cycle Perspective. *Fuel Process. Technol.* **2015**, *132*, 74–82. [CrossRef]
42. Di Marcoberardino, G.; Liao, X.; Dauriat, A.; Binotti, M.; Manzolini, G. Life Cycle Assessment and Economic Analysis of an Innovative Biogas Membrane Reformer for Hydrogen Production. *Processes* **2019**, *7*, 86. [CrossRef]
43. Barana, A.C.; Cereda, M.P. Cassava Wastewater (Manipueira) Treatment Using a Two-Phase Anaerobic Biodigester. *Food Sci. Technol.* **2000**, *20*, 183–186. [CrossRef]
44. Battista, F.; Montenegro Camacho, Y.S.; Hernández, S.; Bensaid, S.; Herrmann, A.; Krause, H.; Trimis, D.; Fino, D. LCA Evaluation for the Hydrogen Production from Biogas through the Innovative BioRobur Project Concept. *Int. J. Hydrog. Energy* **2017**, *42*, 14030–14043. [CrossRef]
45. Li, G.; Wang, S.; Zhao, J.; Qi, H.; Ma, Z.; Cui, P.; Zhu, Z.; Gao, J.; Wang, Y. Life Cycle Assessment and Techno-Economic Analysis of Biomass-to-Hydrogen Production with Methane Tri-Reforming. *Energy* **2020**, *199*, 117488. [CrossRef]
46. Lotrič, A.; Sekavčnik, M.; Kuštrin, I.; Mori, M. Life-Cycle Assessment of Hydrogen Technologies with the Focus on EU Critical Raw Materials and End-of-Life Strategies. *Int. J. Hydrog. Energy* **2021**, *46*, 10143–10160. [CrossRef]
47. Eggemann, L.; Escobar, N.; Peters, R.; Burauel, P.; Stolten, D. Life Cycle Assessment of a Small-Scale Methanol Production System: A Power-to-Fuel Strategy for Biogas Plants. *J. Clean. Prod.* **2020**, *271*, 122476. [CrossRef]
48. Eggemann, L.; Escobar, N.; Peters, R.; Burauel, P.; Stolten, D. Life Cycle Assessment of a Novel Power-To-Fuel System for Methanol Production Using CO<sub>2</sub> From Biogas. In Proceedings of the International Conference on Applied Energy 2019, Västerås, Sweden, 12–15 August 2019; p. 6.
49. Pérez-Fortes, M.; Schöneberger, J.C.; Boulamanti, A.; Tzimas, E. Methanol Synthesis Using Captured CO<sub>2</sub> as Raw Material: Techno-Economic and Environmental Assessment. *Appl. Energy* **2016**, *161*, 718–732. [CrossRef]
50. Azadi, P.; Brownbridge, G.; Mosbach, S.; Smallbone, A.; Bhave, A.; Inderwildi, O.; Kraft, M. The Carbon Footprint and Non-Renewable Energy Demand of Algae-Derived Biodiesel. *Appl. Energy* **2014**, *113*, 1632–1644. [CrossRef]

51. Renó, M.L.G.; Lora, E.E.S.; Palacio, J.C.E.; Venturini, O.J.; Buchgeister, J.; Almazan, O. A LCA (Life Cycle Assessment) of the Methanol Production from Sugarcane Bagasse. *Energy* **2011**, *36*, 3716–3726. [[CrossRef](#)]
52. Iaquaniello, G.; Centi, G.; Salladini, A.; Palo, E.; Perathoner, S.; Spadaccini, L. Waste-to-Methanol: Process and Economics Assessment. *Bioresour. Technol.* **2017**, *243*, 611–619. [[CrossRef](#)] [[PubMed](#)]
53. Schiaroli, N.; Volanti, M.; Crimaldi, A.; Passarini, F.; Vaccari, A.; Fornasari, G.; Copelli, S.; Florit, F.; Lucarelli, C. Biogas to Syngas through the Combined Steam/Dry Reforming Process: An Environmental Impact Assessment. *Energy Fuels* **2021**, *35*, 4224–4236. [[CrossRef](#)]
54. Zeppieri, M.; Villa, P.L.; Verdone, N.; Scarsella, M.; De Filippis, P. Kinetic of Methane Steam Reforming Reaction over Nickel- and Rhodium-Based Catalysts. *Appl. Catal. Gen.* **2010**, *387*, 147–154. [[CrossRef](#)]
55. Papurello, D.; Chiodo, V.; Maisano, S.; Lanzini, A.; Santarelli, M. Catalytic Stability of a Ni-Catalyst towards Biogas Reforming in the Presence of Deactivating Trace Compounds. *Renew. Energy* **2018**, *127*, 481–494. [[CrossRef](#)]
56. Pashchenko, D. Combined Methane Reforming with a Mixture of Methane Combustion Products and Steam over a Ni-Based Catalyst: An Experimental and Thermodynamic Study. *Energy* **2019**, *185*, 573–584. [[CrossRef](#)]
57. Lucrédio, A.F.; Assaf, J.M.; Assaf, E.M. Reforming of a Model Sulfur-Free Biogas on Ni Catalysts Supported on Mg(Al)O Derived from Hydrotalcite Precursors: Effect of La and Rh Addition. *Biomass Bioenergy* **2014**, *60*, 8–17. [[CrossRef](#)]
58. Yentekakis, I.V.; Panagiotopoulou, P.; Artemakis, G. A Review of Recent Efforts to Promote Dry Reforming of Methane (DRM) to Syngas Production via Bimetallic Catalyst Formulations. *Appl. Catal. B Environ.* **2021**, *296*, 120210. [[CrossRef](#)]
59. Rosset, M.; Féris, L.A.; Perez-Lopez, O.W. Biogas Dry Reforming over Ni-M-Al (M = K, Na and Li) Layered Double Hydroxide-Derived Catalysts. *Catal. Today* **2021**, *381*, 96–107. [[CrossRef](#)]
60. Minh, D.P.; Siang, T.J.; Vo, D.-V.N.; Phan, T.S.; Ridart, C.; Nzihou, A.; Grouset, D. Hydrogen Production from Biogas Reforming: An Overview of Steam Reforming, Dry Reforming, Dual Reforming, and Tri-Reforming of Methane. In *Hydrogen Supply Chains: Design, Deployment and Operation*; Azzaro-Pantel, C., Ed.; Elsevier: Amsterdam, The Netherlands, 2018; pp. 111–166.
61. Jabbour, K.; Kaydouh, M.N.; El Hassan, N.; El Zakhem, H.; Casale, S.; Massiani, P.; Davidson, A. Compared Activity and Stability of Three Ni-Silica Catalysts for Methane Bi- and Dry Reforming. In Proceedings of the 2015 International Mediterranean Gas and Oil Conference (MedGO), Mechref, Lebanon, 16–18 April 2015; pp. 1–4.
62. Therdthianwong, S.; Siangchin, C.; Therdthianwong, A. Improvement of Coke Resistance of Ni/Al<sub>2</sub>O<sub>3</sub> Catalyst in CH<sub>4</sub>/CO<sub>2</sub> Reforming by ZrO<sub>2</sub> Addition. *Fuel Process. Technol.* **2008**, *89*, 160–168. [[CrossRef](#)]
63. Benito, M.; García, S.; Ferreira-Aparicio, P.; Serrano, L.G.; Daza, L. Development of Biogas Reforming Ni-La-Al Catalysts for Fuel Cells. *J. Power Source* **2007**, *169*, 177–183. [[CrossRef](#)]
64. Shuyan, W.; Lijie, Y.; Huilin, L.; Yurong, H.; Ding, J.; Guodong, L.; Xiang, L. Simulation of Effect of Catalytic Particle Clustering on Methane Steam Reforming in a Circulating Fluidized Bed Reformer. *Chem. Eng. J.* **2008**, *139*, 136–146. [[CrossRef](#)]
65. Ma, Y.; Xu, Y.; Demura, M.; Hirano, T. Catalytic Stability of Ni<sub>3</sub>Al Powder for Methane Steam Reforming. *Appl. Catal. B Environ.* **2008**, *80*, 15–23. [[CrossRef](#)]
66. Jabbour, K.; Hassan, N.E.; Davidson, A.; Casale, S.; Massiani, P. Factors Affecting the Long-Term Stability of Mesoporous Nickel-Based Catalysts in Combined Steam and Dry Reforming of Methane. *Catal. Sci. Technol.* **2016**, *6*, 4616–4631. [[CrossRef](#)]
67. Samrout, O.E.; Karam, L.; Jabbour, K.; Massiani, P.; Launay, F.; Hassan, N.E. Investigation of New Routes for the Preparation of Mesoporous Calcium Oxide Supported Nickel Materials Used as Catalysts for the Methane Dry Reforming Reaction. *Catal. Sci. Technol.* **2020**, *10*, 6910–6922. [[CrossRef](#)]
68. Lucarelli, C.; Moggi, P.; Cavani, F.; Devillers, M. Sol–Gel Synthesis and Characterization of Transition Metal Based Mixed Oxides and Their Application as Catalysts in Selective Oxidation of Propane. *Appl. Catal. Gen.* **2007**, *325*, 244–250. [[CrossRef](#)]
69. Sun, H.; Wang, H.; Zhang, J. Preparation and Characterization of Nickel–Titanium Composite Xerogel Catalyst for CO<sub>2</sub> Reforming of CH<sub>4</sub>. *Appl. Catal. B Environ.* **2007**, *73*, 158–165. [[CrossRef](#)]
70. Urasaki, K.; Sekine, Y.; Kawabe, S.; Kikuchi, E.; Matsukata, M. Catalytic Activities and Coking Resistance of Ni/Perovskites in Steam Reforming of Methane. *Appl. Catal. Gen.* **2005**, *286*, 23–29. [[CrossRef](#)]
71. Fonseca, A.; Assaf, E.M. Production of the Hydrogen by Methane Steam Reforming over Nickel Catalysts Prepared from Hydrotalcite Precursors. *J. Power Source* **2005**, *142*, 154–159. [[CrossRef](#)]
72. Schiaroli, N.; Lucarelli, C.; Iapalucci, M.C.; Fornasari, G.; Crimaldi, A.; Vaccari, A. Combined Reforming of Clean Biogas over Nanosized Ni–Rh Bimetallic Clusters. *Catalysts* **2020**, *10*, 1345. [[CrossRef](#)]
73. Goula, M.A.; Charisiou, N.D.; Papageridis, K.N.; Delimitis, A.; Pachatouridou, E.; Iliopoulou, E.F. Nickel on Alumina Catalysts for the Production of Hydrogen Rich Mixtures via the Biogas Dry Reforming Reaction: Influence of the Synthesis Method. *Int. J. Hydrog. Energy* **2015**, *40*, 9183–9200. [[CrossRef](#)]
74. Dan, M.; Mihet, M.; Lazar, M.D. Hydrogen and/or Syngas Production by Combined Steam and Dry Reforming of Methane on Nickel Catalysts. *Int. J. Hydrog. Energy* **2020**, *45*, 26254–26264. [[CrossRef](#)]
75. Dan, M.; Mihet, M.; Borodi, G.; Lazar, M.D. Combined Steam and Dry Reforming of Methane for Syngas Production from Biogas Using Bimodal Pore Catalysts. *Catal. Today* **2021**, *366*, 87–96. [[CrossRef](#)]
76. Rego de Vasconcelos, B.; Pham Minh, D.; Lyczko, N.; Phan, T.S.; Sharrock, P.; Nzihou, A. Upgrading Greenhouse Gases (Methane and Carbon Dioxide) into Syngas Using Nickel-Based Catalysts. *Fuel* **2018**, *226*, 195–203. [[CrossRef](#)]
77. Roh, H.-S.; Koo, K.Y.; Jeong, J.H.; Seo, Y.T.; Seo, D.J.; Seo, Y.-S.; Yoon, W.L.; Park, S.B. Combined Reforming of Methane over Supported Ni Catalysts. *Catal. Lett.* **2007**, *117*, 85–90. [[CrossRef](#)]

78. Koo, K.Y.; Roh, H.-S.; Seo, Y.T.; Seo, D.J.; Yoon, W.L.; Park, S.B. Coke Study on MgO-Promoted Ni/Al<sub>2</sub>O<sub>3</sub> Catalyst in Combined H<sub>2</sub>O and CO<sub>2</sub> Reforming of Methane for Gas to Liquid (GTL) Process. *Appl. Catal. Gen.* **2008**, *340*, 183–190. [[CrossRef](#)]
79. Olah, G.A.; Prakash, G.K.S. Conversion of Carbon Dioxide to Methanol and/or Dimethyl Ether Using Bi-Reforming of Methane or Natural Gas. U.S. Patent US7906559B2, 15 March 2011.
80. Effendi, A.; Hellgardt, K.; Zhang, Z.-G.; Yoshida, T. Optimising H<sub>2</sub> Production from Model Biogas via Combined Steam Reforming and CO Shift Reactions. *Fuel* **2005**, *84*, 869–874. [[CrossRef](#)]
81. Villacampa, J.I.; Royo, C.; Romeo, E.; Montoya, J.A.; Del Angel, P.; Monzón, A. Catalytic Decomposition of Methane over Ni-Al<sub>2</sub>O<sub>3</sub> Coprecipitated Catalysts: Reaction and Regeneration Studies. *Appl. Catal. Gen.* **2003**, *252*, 363–383. [[CrossRef](#)]
82. Tuna, C.E.; Silveira, J.L.; da Silva, M.E.; Boloy, R.M.; Braga, L.B.; Pérez, N.P. Biogas Steam Reformer for Hydrogen Production: Evaluation of the Reformer Prototype and Catalysts. *Int. J. Hydrog. Energy* **2018**, *43*, 2108–2120. [[CrossRef](#)]
83. Karam, L.; Reboul, J.; Casale, S.; Massiani, P.; El Hassan, N. Porous Nickel-Alumina Derived from Metal-Organic Framework (MIL-53): A New Approach to Achieve Active and Stable Catalysts in Methane Dry Reforming. *ChemCatChem* **2020**, *12*, 373–385. [[CrossRef](#)]
84. Olah, G.A.; Prakash, G.K.S. Efficient, Self Sufficient Production of Methanol from a Methane Source via Oxidative Bi-Reforming. U.S. Patent AU2013330420B2, 17 October 2016.
85. Roh, H.-S.; Koo, K.Y.; Joshi, U.D.; Yoon, W.L. Combined H<sub>2</sub>O and CO<sub>2</sub> Reforming of Methane Over Ni-Ce-ZrO<sub>2</sub> Catalysts for Gas to Liquids (GTL). *Catal. Lett.* **2008**, *125*, 283–288. [[CrossRef](#)]
86. Yin, W.; Guilhaume, N.; Schuurman, Y. Model Biogas Reforming over Ni-Rh/MgAl<sub>2</sub>O<sub>4</sub> Catalyst. Effect of Gas Impurities. *Chem. Eng. J.* **2020**, *398*, 125534. [[CrossRef](#)]
87. Lee, J.H.; Koo, K.Y.; Jung, U.H.; Park, J.E.; Yoon, W.L. The Promotional Effect of K on the Catalytic Activity of Ni/MgAl<sub>2</sub>O<sub>4</sub> for the Combined H<sub>2</sub>O and CO<sub>2</sub> Reforming of Coke Oven Gas for Syngas Production. *Korean J. Chem. Eng.* **2016**, *33*, 3115–3120. [[CrossRef](#)]
88. Pham, X.-H.; Ashik, U.P.M.; Hayashi, J.-I.; Pérez Alonso, A.; Pla, D.; Gómez, M.; Pham Minh, D. Review on the Catalytic Tri-Reforming of Methane—Part II: Catalyst Development. *Appl. Catal. Gen.* **2021**, *623*, 118286. [[CrossRef](#)]
89. Zhang, R.; Xia, G.; Li, M.; Wu, Y.; Nie, H.; Li, D. Effect of Support on the Performance of Ni-Based Catalyst in Methane Dry Reforming. *J. Fuel Chem. Technol.* **2015**, *43*, 1359–1365. [[CrossRef](#)]
90. Omoregbe, O.; Danh, H.T.; Nguyen-Huy, C.; Setiabudi, H.D.; Abidin, S.Z.; Truong, Q.D.; Vo, D.-V.N. Syngas Production from Methane Dry Reforming over Ni/SBA-15 Catalyst: Effect of Operating Parameters. *Int. J. Hydrog. Energy* **2017**, *42*, 11283–11294. [[CrossRef](#)]
91. Xie, T.; Zhao, X.; Zhang, J.; Shi, L.; Zhang, D. Ni Nanoparticles Immobilized Ce-Modified Mesoporous Silica via a Novel Sublimation-Deposition Strategy for Catalytic Reforming of Methane with Carbon Dioxide. *Int. J. Hydrog. Energy* **2015**, *40*, 9685–9695. [[CrossRef](#)]
92. Zhang, S.; Muratsugu, S.; Ishiguro, N.; Tada, M. Ceria-Doped Ni/SBA-16 Catalysts for Dry Reforming of Methane. *ACS Catal.* **2013**, *3*, 1855–1864. [[CrossRef](#)]
93. Daoura, O.; Boutros, M.; Launay, F. Ni-Silica-Based Catalysts for CH<sub>4</sub> Reforming by CO<sub>2</sub> with Enhanced Stability: Recent Designs and the Impacts of Ni Confinement, Promoters, and Core-Shell Structures. *J. Energy Power Technol.* **2021**, *3*, 38. [[CrossRef](#)]
94. Majewski, A.J.; Wood, J. Tri-Reforming of Methane over Ni@SiO<sub>2</sub> Catalyst. *Int. J. Hydrog. Energy* **2014**, *39*, 12578–12585. [[CrossRef](#)]
95. Lim, Z.-Y.; Tu, J.; Xu, Y.; Chen, B. Ni@ZrO<sub>2</sub> yolk-shell catalyst for CO<sub>2</sub> methane reforming: Effect of Ni@SiO<sub>2</sub> size as the hard-template. *J. Colloid Interface Sci.* **2021**, *590*, 641–651. [[CrossRef](#)]
96. Singha, R.K.; Shukla, A.; Yadav, A.; Adak, S.; Iqbal, Z.; Siddiqui, N.; Bal, R. Energy Efficient Methane Tri-Reforming for Synthesis Gas Production over Highly Coke Resistant Nanocrystalline Ni-ZrO<sub>2</sub> Catalyst. *Appl. Energy* **2016**, *178*, 110–125. [[CrossRef](#)]
97. Barroso-Quiroga, M.M.; Castro-Luna, A.E. Catalytic Activity and Effect of Modifiers on Ni-Based Catalysts for the Dry Reforming of Methane. *Int. J. Hydrog. Energy* **2010**, *35*, 6052–6056. [[CrossRef](#)]
98. Deng, J.; Bu, K.; Shen, Y.; Zhang, X.; Zhang, J.; Faungnawakij, K.; Zhang, D. Cooperatively Enhanced Coking Resistance via Boron Nitride Coating over Ni-Based Catalysts for Dry Reforming of Methane. *Appl. Catal. B Environ.* **2022**, *302*, 120859. [[CrossRef](#)]
99. Tran, T.Q.; Pham Minh, D.; Phan, T.S.; Pham, Q.N.; Nguyen Xuan, H. Dry Reforming of Methane over Calcium-Deficient Hydroxyapatite Supported Cobalt and Nickel Catalysts. *Chem. Eng. Sci.* **2020**, *228*, 115975. [[CrossRef](#)]
100. Rego de Vasconcelos, B.; Pham Minh, D.; Martins, E.; Germeau, A.; Sharrock, P.; Nzihou, A. Highly-Efficient Hydroxyapatite-Supported Nickel Catalysts for Dry Reforming of Methane. *Int. J. Hydrog. Energy* **2020**, *45*, 18502–18518. [[CrossRef](#)]
101. Phan, T.S.; Sane, A.R.; Rêgo de Vasconcelos, B.; Nzihou, A.; Sharrock, P.; Grouset, D.; Pham Minh, D. Hydroxyapatite Supported Bimetallic Cobalt and Nickel Catalysts for Syngas Production from Dry Reforming of Methane. *Appl. Catal. B Environ.* **2018**, *224*, 310–321. [[CrossRef](#)]
102. Rego de Vasconcelos, B.; Pham Minh, D.; Sharrock, P.; Nzihou, A. Regeneration Study of Ni/Hydroxyapatite Spent Catalyst from Dry Reforming. *Catal. Today* **2018**, *310*, 107–115. [[CrossRef](#)]
103. Roshia, P.; Mohapatra, S.K.; Mahla, S.K.; Dhir, A. Catalytic Reforming of Synthetic Biogas for Hydrogen Enrichment over Ni Supported on ZnOCeO<sub>2</sub> Mixed Catalyst. *Biomass Bioenergy* **2019**, *125*, 70–78. [[CrossRef](#)]
104. Iglesias, I.; Forti, M.; Baronetti, G.; Mariño, F. Zr-Enhanced Stability of Ceria Based Supports for Methane Steam Reforming at Severe Reaction Conditions. *Int. J. Hydrog. Energy* **2019**, *44*, 8121–8132. [[CrossRef](#)]



105. Vita, A.; Pino, L.; Cipiti, F.; Laganà, M.; Recupero, V. Biogas as Renewable Raw Material for Syngas Production by Tri-Reforming Process over NiCeO<sub>2</sub> Catalysts: Optimal Operative Condition and Effect of Nickel Content. *Fuel Process. Technol.* **2014**, *127*, 47–58. [[CrossRef](#)]
106. Park, M.-J.; Kim, J.-H.; Lee, Y.-H.; Kim, H.-M.; Jeong, D.-W. System Optimization for Effective Hydrogen Production via Anaerobic Digestion and Biogas Steam Reforming. *Int. J. Hydrog. Energy* **2020**, *45*, 30188–30200. [[CrossRef](#)]
107. Deng, J.; Chu, W.; Wang, B.; Yang, W.; Zhao, X.S. Mesoporous Ni/Ce 1-x Ni x O 2-y Heterostructure as an Efficient Catalyst for Converting Greenhouse Gas to H<sub>2</sub> and Syngas. *Catal. Sci. Technol.* **2016**, *6*, 851–862. [[CrossRef](#)]
108. Chen, X.; Yik, E.; Butler, J.; Schwank, J.W. Gasification Characteristics of Carbon Species Derived from Model Reforming Compound over Ni/Ce-Zr-O Catalysts. *Catal. Today* **2014**, *233*, 14–20. [[CrossRef](#)]
109. Al-Swai, B.M.; Osman, N.B.; Ramli, A.; Abdullah, B.; Farooqi, A.S.; Ayodele, B.V.; Patrick, D.O. Low-Temperature Catalytic Conversion of Greenhouse Gases (CO<sub>2</sub> and CH<sub>4</sub>) to Syngas over Ceria-Magnesia Mixed Oxide Supported Nickel Catalysts. *Int. J. Hydrog. Energy* **2021**, *46*, 24768–24780. [[CrossRef](#)]
110. Djinović, P.; Osojnik Črnivec, I.G.; Erjavec, B.; Pintar, A. Influence of Active Metal Loading and Oxygen Mobility on Coke-Free Dry Reforming of Ni-Co Bimetallic Catalysts. *Appl. Catal. B Environ.* **2012**, *125*, 259–270. [[CrossRef](#)]
111. Yao, L.; Shi, J.; Xu, H.; Shen, W.; Hu, C. Low-Temperature CO<sub>2</sub> Reforming of Methane on Zr-Promoted Ni/SiO<sub>2</sub> Catalyst. *Fuel Process. Technol.* **2016**, *144*, 1–7. [[CrossRef](#)]
112. Das, S.; Ashok, J.; Bian, Z.; Dewangan, N.; Wai, M.H.; Du, Y.; Borgna, A.; Hidajat, K.; Kawi, S. Silica-Ceria Sandwiched Ni Core-Shell Catalyst for Low Temperature Dry Reforming of Biogas: Coke Resistance and Mechanistic Insights. *Appl. Catal. B Environ.* **2018**, *230*, 220–236. [[CrossRef](#)]
113. Marinho, A.L.A.; Rabelo-Neto, R.C.; Epron, F.; Bion, N.; Noronha, F.B.; Toniolo, F.S. Pt Nanoparticles Embedded in CeO<sub>2</sub> and CeZrO<sub>2</sub> Catalysts for Biogas Upgrading: Investigation on Carbon Removal Mechanism by Oxygen Isotopic Exchange and DRIFTS. *J. CO<sub>2</sub> Util.* **2021**, *49*, 101572. [[CrossRef](#)]
114. Gao, N.; Cheng, M.; Quan, C.; Zheng, Y. Syngas Production via Combined Dry and Steam Reforming of Methane over Ni-Ce/ZSM-5 Catalyst. *Fuel* **2020**, *273*, 117702. [[CrossRef](#)]
115. Slagtern, A.; Schuurman, Y.; Leclercq, C.; Verykios, X.; Mirodatos, C. Specific Features Concerning the Mechanism of Methane Reforming by Carbon Dioxide over Ni/La<sub>2</sub>O<sub>3</sub> Catalyst. *J. Catal.* **1997**, *172*, 118–126. [[CrossRef](#)]
116. Tsipouriari, V.A.; Verykios, X.E. Carbon and Oxygen Reaction Pathways of CO<sub>2</sub> Reforming of Methane over Ni/La<sub>2</sub>O<sub>3</sub> and Ni/Al<sub>2</sub>O<sub>3</sub> Catalysts Studied by Isotopic Tracing Techniques. *J. Catal.* **1999**, *187*, 85–94. [[CrossRef](#)]
117. Charisiou, N.D.; Siakavelas, G.; Tzounis, L.; Sebastian, V.; Monzon, A.; Baker, M.A.; Hinder, S.J.; Polychronopoulou, K.; Yentekakis, I.V.; Goula, M.A. An in Depth Investigation of Deactivation through Carbon Formation during the Biogas Dry Reforming Reaction for Ni Supported on Modified with CeO<sub>2</sub> and La<sub>2</sub>O<sub>3</sub> Zirconia Catalysts. *Int. J. Hydrog. Energy* **2018**, *43*, 18955–18976. [[CrossRef](#)]
118. Angeli, S.D.; Turchetti, L.; Monteleone, G.; Lemonidou, A.A. Catalyst Development for Steam Reforming of Methane and Model Biogas at Low Temperature. *Appl. Catal. B Environ.* **2016**, *181*, 34–46. [[CrossRef](#)]
119. Matsumura, Y.; Nakamori, T. Steam Reforming of Methane over Nickel Catalysts at Low Reaction Temperature. *Appl. Catal. Gen.* **2004**, *258*, 107–114. [[CrossRef](#)]
120. Moura, J.S.; Fonseca, J.D.S.L.; Bion, N.; Epron, F.; de Freitas Silva, T.; Maciel, C.G.; Assaf, J.M.; do Carmo Rangel, M. Effect of Lanthanum on the Properties of Copper, Cerium and Zirconium Catalysts for Preferential Oxidation of Carbon Monoxide. *Catal. Today* **2014**, *228*, 40–50. [[CrossRef](#)]
121. Hennings, U.; Reimert, R. Noble Metal Catalysts Supported on Gadolinium Doped Ceria Used for Natural Gas Reforming in Fuel Cell Applications. *Appl. Catal. B Environ.* **2007**, *70*, 498–508. [[CrossRef](#)]
122. Zou, Q.; Zhao, Y.; Jin, X.; Fang, J.; Li, D.; Li, K.; Lu, J.; Luo, Y. Ceria-Nano Supported Copper Oxide Catalysts for CO Preferential Oxidation: Importance of Oxygen Species and Metal-Support Interaction. *Appl. Surf. Sci.* **2019**, *494*, 1166–1176. [[CrossRef](#)]
123. Teh, L.P.; Setiabudi, H.D.; Timmiati, S.N.; Aziz, M.A.A.; Annuar, N.H.R.; Ruslan, N.N. Recent Progress in Ceria-Based Catalysts for the Dry Reforming of Methane: A Review. *Chem. Eng. Sci.* **2021**, *242*, 116606. [[CrossRef](#)]
124. Fornasiero, P.; Dimonte, R.; Rao, G.R.; Kaspar, J.; Meriani, S.; Trovarelli, A.; Graziani, M. Rh-Loaded CeO<sub>2</sub>-ZrO<sub>2</sub> Solid-Solutions as Highly Efficient Oxygen Exchangers: Dependence of the Reduction Behavior and the Oxygen Storage Capacity on the Structural-Properties. *J. Catal.* **1995**, *151*, 168–177. [[CrossRef](#)]
125. Ozawa, M.; Takahashi-Morita, M.; Kobayashi, K.; Haneda, M. Core-Shell Type Ceria Zirconia Support for Platinum and Rhodium Three Way Catalysts. *Catal. Today* **2017**, *281*, 482–489. [[CrossRef](#)]
126. Valderrama, G.; Kiennemann, A.; Goldwasser, M.R. La-Sr-Ni-Co-O Based Perovskite-Type Solid Solutions as Catalyst Precursors in the CO<sub>2</sub> Reforming of Methane. *J. Power Source* **2010**, *195*, 1765–1771. [[CrossRef](#)]
127. Rivas, M.E.; Fierro, J.L.G.; Goldwasser, M.R.; Pietri, E.; Pérez-Zurita, M.J.; Griboval-Constant, A.; Leclercq, G. Structural Features and Performance of LaNi<sub>1-x</sub>Rh<sub>x</sub>O<sub>3</sub> System for the Dry Reforming of Methane. *Appl. Catal. Gen.* **2008**, *344*, 10–19. [[CrossRef](#)]
128. Nam, J.W.; Chae, H.; Lee, S.H.; Jung, H.; Lee, K.-Y. Methane Dry Reforming over Well-Dispersed Ni Catalyst Prepared from Perovskite-Type Mixed Oxides. In *Studies in Surface Science and Catalysis, Natural Gas Conversion V*; Parmaliana, A., Sanfilippo, D., Frusteri, F., Vaccari, A., Arena, F., Eds.; Elsevier: Amsterdam, The Netherlands, 1998; Volume 119, pp. 843–848.
129. Yang, E.; Noh, Y.; Ramesh, S.; Lim, S.S.; Moon, D.J. The Effect of Promoters in La<sub>0.9</sub>M<sub>0.1</sub>Ni<sub>0.5</sub>Fe<sub>0.5</sub>O<sub>3</sub> (M=Sr, Ca) Perovskite Catalysts on Dry Reforming of Methane. *Fuel Process. Technol.* **2015**, *134*, 404–413. [[CrossRef](#)]

130. Moradi, G.R.; Rahmanzadeh, M.; Khosravian, F. The Effects of Partial Substitution of Ni by Zn in LaNiO<sub>3</sub> Perovskite Catalyst for Methane Dry Reforming. *J. CO<sub>2</sub> Util.* **2014**, *6*, 7–11. [[CrossRef](#)]
131. Su, Y.-J.; Pan, K.-L.; Chang, M.-B. Modifying Perovskite-Type Oxide Catalyst LaNiO<sub>3</sub> with Ce for Carbon Dioxide Reforming of Methane. *Int. J. Hydrog. Energy* **2014**, *39*, 4917–4925. [[CrossRef](#)]
132. de Lima, S.M.; Pena, M.A.; Fierro, J.L.G.; Assaf, J.M. La<sub>1-x</sub>Ca<sub>x</sub>NiO<sub>3</sub> Perovskite Oxides: Characterization and Catalytic Reactivity in Dry Reforming of Methane. *Catal. Lett.* **2008**, *124*, 195–203. [[CrossRef](#)]
133. Kim, W.Y.; Jang, J.S.; Ra, E.C.; Kim, K.Y.; Kim, E.H.; Lee, J.S. Reduced Perovskite LaNiO<sub>3</sub> Catalysts Modified with Co and Mn for Low Coke Formation in Dry Reforming of Methane. *Appl. Catal. Gen.* **2019**, *575*, 198–203. [[CrossRef](#)]
134. Yang, E.; Noh, Y.S.; Hong, G.H.; Moon, D.J. Combined Steam and CO<sub>2</sub> Reforming of Methane over La<sub>1-x</sub>Sr<sub>x</sub>NiO<sub>3</sub> Perovskite Oxides. *Catal. Today* **2018**, *299*, 242–250. [[CrossRef](#)]
135. Lucarelli, C.; Molinari, C.; Faure, R.; Fornasari, G.; Gary, D.; Schiaroli, N.; Vaccari, A. Novel Cu-Zn-Al Catalysts Obtained from Hydrotalcite-Type Precursors for Middle-Temperature Water-Gas Shift Applications. *Appl. Clay Sci.* **2018**, *155*, 103–110. [[CrossRef](#)]
136. Gogate, M.R. Methanol Synthesis Revisited: The Nature of the Active Site of Cu in Industrial Cu/ZnO/Al<sub>2</sub>O<sub>3</sub> Catalyst and Cu-Zn Synergy. *Pet. Sci. Technol.* **2019**, *37*, 671–678. [[CrossRef](#)]
137. Sokolov, S.; Radnik, J.; Schneider, M.; Rodemerck, U. Low-Temperature CO<sub>2</sub> Reforming of Methane over Ni Supported on ZnAl Mixed Metal Oxides. *Int. J. Hydrog. Energy* **2017**, *42*, 9831–9839. [[CrossRef](#)]
138. Park, J.-H.; Yeo, S.; Kang, T.-J.; Shin, H.-R.; Heo, I.; Chang, T.-S. Effect of Zn Promoter on Catalytic Activity and Stability of Co/ZrO<sub>2</sub> Catalyst for Dry Reforming of CH<sub>4</sub>. *J. CO<sub>2</sub> Util.* **2018**, *23*, 10–19. [[CrossRef](#)]
139. Cunha, A.F.; Morales-Torres, S.; Pastrana-Martínez, L.M.; Maldonado-Hódar, F.J.; Caetano, N.S. Syngas Production by Bi-Reforming of Methane on a Bimetallic Ni-ZnO Doped Zeolite 13X. *Fuel* **2021**, *311*, 122592. [[CrossRef](#)]
140. Chatla, A.; Abu-Rub, F.; Prakash, A.V.; Ibrahim, G.; Elbashir, N.O. Highly Stable and Coke-Resistant Zn-Modified Ni-Mg-Al Hydrotalcite Derived Catalyst for Dry Reforming of Methane: Synergistic Effect of Ni and Zn. *Fuel* **2022**, *308*, 122042. [[CrossRef](#)]
141. Anjaneyulu, C.; da Costa, L.O.O.; Ribeiro, M.C.; Rabelo-Neto, R.C.; Mattos, L.V.; Venugopal, A.; Noronha, F.B. Effect of Zn Addition on the Performance of Ni/Al<sub>2</sub>O<sub>3</sub> Catalyst for Steam Reforming of Ethanol. *Appl. Catal. Gen.* **2016**, *519*, 85–98. [[CrossRef](#)]
142. Ma, W.; Xie, M.; Xie, S.; Wei, L.; Cai, Y.; Zhang, Q.; Wang, Y. Nickel and Indium Core-Shell Co-Catalysts Loaded Silicon Nanowire Arrays for Efficient Photoelectrocatalytic Reduction of CO<sub>2</sub> to Formate. *J. Energy Chem.* **2021**, *54*, 422–428. [[CrossRef](#)]
143. Shen, C.; Bao, Q.; Xue, W.; Sun, K.; Zhang, Z.; Jia, X.; Mei, D.; Liu, C. Synergistic Effect of the Metal-Support Interaction and Interfacial Oxygen Vacancy for CO<sub>2</sub> Hydrogenation to Methanol over Ni/In<sub>2</sub>O<sub>3</sub> Catalyst: A Theoretical Study. *J. Energy Chem.* **2022**, *65*, 623–629. [[CrossRef](#)]
144. Frei, M.S.; Mondelli, C.; García-Muelas, R.; Morales-Vidal, J.; Philipp, M.; Safonova, O.V.; López, N.; Stewart, J.A.; Ferré, D.C.; Pérez-Ramírez, J. Nanostructure of Nickel-Promoted Indium Oxide Catalysts Drives Selectivity in CO<sub>2</sub> Hydrogenation. *Nat. Commun.* **2021**, *12*, 1960. [[CrossRef](#)]
145. Horváth, A.; Németh, M.; Beck, A.; Maróti, B.; Sáfrán, G.; Pantaleo, G.; Liotta, L.F.; Venezia, A.M.; La Parola, V. Strong Impact of Indium Promoter on Ni/Al<sub>2</sub>O<sub>3</sub> and Ni/CeO<sub>2</sub>-Al<sub>2</sub>O<sub>3</sub> Catalysts Used in Dry Reforming of Methane. *Appl. Catal. Gen.* **2021**, *621*, 118174. [[CrossRef](#)]
146. Liu, W.; Li, L.; Lin, S.; Luo, Y.; Bao, Z.; Mao, Y.; Li, K.; Wu, D.; Peng, H. Confined Ni-In Intermetallic Alloy Nanocatalyst with Excellent Coking Resistance for Methane Dry Reforming. *J. Energy Chem.* **2022**, *65*, 34–47. [[CrossRef](#)]
147. Pakhare, D.; Spivey, J. A Review of Dry (CO<sub>2</sub>) Reforming of Methane over Noble Metal Catalysts. *Chem. Soc. Rev.* **2014**, *43*, 7813–7837. [[CrossRef](#)] [[PubMed](#)]
148. Aramouni, N.A.K.; Touma, J.G.; Tarboush, B.A.; Zeaiter, J.; Ahmad, M.N. Catalyst Design for Dry Reforming of Methane: Analysis Review. *Renew. Sustain. Energy Rev.* **2018**, *82*, 2570–2585. [[CrossRef](#)]
149. Großmann, K.; Dellermann, T.; Dillig, M.; Karl, J. Coking Behavior of Nickel and a Rhodium Based Catalyst Used in Steam Reforming for Power-to-Gas Applications. *Int. J. Hydrog. Energy* **2017**, *42*, 11150–11158. [[CrossRef](#)]
150. Cimino, S.; Lisi, L.; Mancino, G. Effect of Phosphorous Addition to Rh-Supported Catalysts for the Dry Reforming of Methane. *Int. J. Hydrog. Energy* **2017**, *42*, 23587–23598. [[CrossRef](#)]
151. Ho, P.H.; Ospitali, F.; Sanghez de Luna, G.; Fornasari, G.; Vaccari, A.; Benito, P. Coating of Rh/Mg/Al Hydrotalcite-Like Materials on FeCrAl Fibers by Electrodeposition and Application for Syngas Production. *Energy Technol.* **2020**, *8*, 1901018. [[CrossRef](#)]
152. Fasolini, A.; Abate, S.; Barbera, D.; Centi, G.; Basile, F. Pure H<sub>2</sub> Production by Methane Oxy-Reforming over Rh-Mg-Al Hydrotalcite-Derived Catalysts Coupled with a Pd Membrane. *Appl. Catal. Gen.* **2019**, *581*, 91–102. [[CrossRef](#)]
153. Yentekakis, I.V.; Goula, G.; Hatzisymeon, M.; Betsi-Argyropoulou, I.; Botzolaki, G.; Kousi, K.; Kondarides, D.I.; Taylor, M.J.; Parlett, C.M.A.; Osatiashtiani, A.; et al. Effect of Support Oxygen Storage Capacity on the Catalytic Performance of Rh Nanoparticles for CO<sub>2</sub> Reforming of Methane. *Appl. Catal. B Environ.* **2019**, *243*, 490–501. [[CrossRef](#)]
154. Moral, A.; Reyero, I.; Alfaro, C.; Bimbela, F.; Gandía, L.M. Syngas Production by Means of Biogas Catalytic Partial Oxidation and Dry Reforming Using Rh-Based Catalysts. *Catal. Today* **2018**, *299*, 280–288. [[CrossRef](#)]
155. de Caprariis, B.; de Filippis, P.; Palma, V.; Petrullo, A.; Ricca, A.; Ruocco, C.; Scarsella, M. Rh, Ru and Pt Ternary Perovskites Type Oxides BaZr<sub>(1-x)</sub>MexO<sub>3</sub> for Methane Dry Reforming. *Appl. Catal. Gen.* **2016**, *517*, 47–55. [[CrossRef](#)]
156. Bradford, M.C.J.; Vannice, M.A. CO<sub>2</sub> Reforming of CH<sub>4</sub> over Supported Ru Catalysts. *J. Catal.* **1999**, *183*, 69–75. [[CrossRef](#)]
157. Matsui, N.; Nakagawa, K.; Ikenaga, N.; Suzuki, T. Reactivity of Carbon Species Formed on Supported Noble Metal Catalysts in Methane Conversion Reactions. *J. Catal.* **2000**, *194*, 115–121. [[CrossRef](#)]

158. Sutton, D.; Parle, S.M.; Ross, J.R.H. The CO<sub>2</sub> Reforming of the Hydrocarbons Present in a Model Gas Stream over Selected Catalysts. *Fuel Process. Technol.* **2002**, *75*, 45–53. [[CrossRef](#)]
159. Qin, D.; Lapszewicz, J. Study of Mixed Steam and CO<sub>2</sub> Reforming of CH<sub>4</sub> to Syngas on MgO-Supported Metals. *Catal. Today* **1994**, *21*, 551–560. [[CrossRef](#)]
160. Egawa, C. Methane Dry Reforming Reaction on Ru(001) Surfaces. *J. Catal.* **2018**, *358*, 35–42. [[CrossRef](#)]
161. Wang, W.-Y.; Wang, G.-C. The First-Principles-Based Microkinetic Simulation of the Dry Reforming of Methane over Ru(0001). *Catal. Sci. Technol.* **2021**, *11*, 1395–1406. [[CrossRef](#)]
162. Lee, C.H.; Kwon, B.W.; Oh, J.H.; Kim, S.; Han, J.; Nam, S.W.; Yoon, S.P.; Lee, K.B.; Ham, H.C. Integration of Dry-Reforming and Sorption-Enhanced Water Gas Shift Reactions for the Efficient Production of High-Purity Hydrogen from Anthropogenic Greenhouse Gases. *J. Ind. Eng. Chem.* **2022**, *105*, 563–570. [[CrossRef](#)]
163. da Fonseca, R.O.; Rabelo-Neto, R.C.; Simões, R.C.C.; Mattos, L.V.; Noronha, F.B. Pt Supported on Doped CeO<sub>2</sub>/Al<sub>2</sub>O<sub>3</sub> as Catalyst for Dry Reforming of Methane. *Int. J. Hydrog. Energy* **2020**, *45*, 5182–5191. [[CrossRef](#)]
164. Izquierdo, U.; Barrio, V.L.; Bizkarra, K.; Gutierrez, A.M.; Arraibi, J.R.; Gartzia, L.; Bañuelos, J.; Lopez-Arbeloa, I.; Cambra, J.F. Ni and RhNi Catalysts Supported on Zeolites L for Hydrogen and Syngas Production by Biogas Reforming Processes. *Chem. Eng. J.* **2014**, *238*, 178–188. [[CrossRef](#)]
165. Jóźwiak, W.K.; Nowosielska, M.; Rynkowski, J. Reforming of Methane with Carbon Dioxide over Supported Bimetallic Catalysts Containing Ni and Noble Metal: I. Characterization and Activity of SiO<sub>2</sub> Supported Ni–Rh Catalysts. *Appl. Catal. Gen.* **2005**, *280*, 233–244. [[CrossRef](#)]
166. Horváth, A.; Stefler, G.; Geszti, O.; Kienneman, A.; Pietraszek, A.; Guzzi, L. Methane Dry Reforming with CO<sub>2</sub> on CeZr-Oxide Supported Ni, NiRh and NiCo Catalysts Prepared by Sol–Gel Technique: Relationship between Activity and Coke Formation. *Catal. Today* **2011**, *169*, 102–111. [[CrossRef](#)]
167. Hou, Z.; Chen, P.; Fang, H.; Zheng, X.; Yashima, T. Production of Synthesis Gas via Methane Reforming with CO<sub>2</sub> on Noble Metals and Small Amount of Noble-(Rh-) Promoted Ni Catalysts. *Int. J. Hydrog. Energy* **2006**, *31*, 555–561. [[CrossRef](#)]
168. García-Diéguez, M.; Pieta, I.S.; Herrera, M.C.; Larrubia, M.A.; Alemany, L.J. RhNi Nanocatalysts for the CO<sub>2</sub> and CO<sub>2</sub>+H<sub>2</sub>O Reforming of Methane. *Catal. Today* **2011**, *172*, 136–142. [[CrossRef](#)]
169. Schiaroli, N.; Lucarelli, C.; Sanghez de Luna, G.; Fornasari, G.; Vaccari, A. Ni-Based Catalysts to Produce Synthesis Gas by Combined Reforming of Clean Biogas. *Appl. Catal. Gen.* **2019**, *582*, 117087. [[CrossRef](#)]
170. Álvarez, M.A.; Centeno, M.A.; Odriozola, J.A. Ru–Ni Catalyst in the Combined Dry-Steam Reforming of Methane: The Importance in the Metal Order Addition. *Top. Catal.* **2016**, *59*, 303–313. [[CrossRef](#)]
171. Zhou, H.; Zhang, T.; Sui, Z.; Zhu, Y.-A.; Han, C.; Zhu, K.; Zhou, X. A Single Source Method to Generate Ru-Ni-MgO Catalysts for Methane Dry Reforming and the Kinetic Effect of Ru on Carbon Deposition and Gasification. *Appl. Catal. B Environ.* **2018**, *233*, 143–159. [[CrossRef](#)]
172. Xu, Y.; Li, J.; Jiang, F.; Xu, Y.; Liu, B.; Liu, X. Insight into the Anti-Coking Ability of NiM/SiO<sub>2</sub> (M=ZrO<sub>2</sub>, Ru) Catalyst for Dry Reforming of CH<sub>4</sub> to Syngas. *Int. J. Hydrog. Energy* **2021**, *47*, 2268–2278. [[CrossRef](#)]
173. Batebi, D.; Abedini, R.; Mosayebi, A. Combined Steam and CO<sub>2</sub> Reforming of Methane (CSCRM) over Ni–Pd/Al<sub>2</sub>O<sub>3</sub> Catalyst for Syngas Formation. *Int. J. Hydrog. Energy* **2020**, *45*, 14293–14310. [[CrossRef](#)]
174. Pan, C.; Guo, Z.; Dai, H.; Ren, R.; Chu, W. Anti-Sintering Mesoporous Ni–Pd Bimetallic Catalysts for Hydrogen Production via Dry Reforming of Methane. *Int. J. Hydrog. Energy* **2020**, *45*, 16133–16143. [[CrossRef](#)]
175. Chein, R.; Yang, Z. Experimental Study on Dry Reforming of Biogas for Syngas Production over Ni-Based Catalysts. *ACS Omega* **2019**, *4*, 20911–20922. [[CrossRef](#)]
176. Li, L.; Zhou, L.; Ould-Chikh, S.; Anjum, D.H.; Kanoun, M.B.; Scaranto, J.; Hedhili, M.N.; Khalid, S.; Laveille, P.V.; D’Souza, L.; et al. Controlled Surface Segregation Leads to Efficient Coke-Resistant Nickel/Platinum Bimetallic Catalysts for the Dry Reforming of Methane. *ChemCatChem* **2015**, *7*, 819–829. [[CrossRef](#)]
177. Wu, Z.; Yang, B.; Miao, S.; Liu, W.; Xie, J.; Lee, S.; Pellin, M.J.; Xiao, D.; Su, D.; Ma, D. Lattice Strained Ni-Co Alloy as a High-Performance Catalyst for Catalytic Dry Reforming of Methane. *ACS Catal.* **2019**, *9*, 2693–2700. [[CrossRef](#)]
178. Xu, J.; Zhou, W.; Li, Z.; Wang, J.; Ma, J. Biogas Reforming for Hydrogen Production over Nickel and Cobalt Bimetallic Catalysts. *Int. J. Hydrog. Energy* **2009**, *34*, 6646–6654. [[CrossRef](#)]
179. Zhang, J.; Wang, H.; Dalai, A.K. Development of Stable Bimetallic Catalysts for Carbon Dioxide Reforming of Methane. *J. Catal.* **2007**, *249*, 300–310. [[CrossRef](#)]
180. Fan, X.; Liu, Z.; Zhu, Y.-A.; Tong, G.; Zhang, J.; Engelbrekt, C.; Ulstrup, J.; Zhu, K.; Zhou, X. Tuning the Composition of Metastable CoxNiyMg100–x–y(OH)(OCH<sub>3</sub>) Nanoplates for Optimizing Robust Methane Dry Reforming Catalyst. *J. Catal.* **2015**, *330*, 106–119. [[CrossRef](#)]
181. Beheshti Askari, A.; al Samarai, M.; Morana, B.; Tillmann, L.; Pfänder, N.; Wandzilak, A.; Watts, B.; Belkhou, R.; Muhler, M.; DeBeer, S. In Situ X-ray Microscopy Reveals Particle Dynamics in a NiCo Dry Methane Reforming Catalyst under Operating Conditions. *ACS Catal.* **2020**, *10*, 6223–6230. [[CrossRef](#)]
182. Theofanidis, S.A.; Galvita, V.V.; Poelman, H.; Marin, G.B. Enhanced Carbon-Resistant Dry Reforming Fe-Ni Catalyst: Role of Fe. *ACS Catal.* **2015**, *5*, 3028–3039. [[CrossRef](#)]

183. De Coster, V.; Srinath, N.V.; Theofanidis, S.A.; Pirro, L.; Van Alboom, A.; Poelman, H.; Sabbe, M.K.; Marin, G.B.; Galvita, V.V. Looking inside a Ni-Fe/MgAl<sub>2</sub>O<sub>4</sub> Catalyst for Methane Dry Reforming via Mössbauer Spectroscopy and in Situ QXAS. *Appl. Catal. B Environ.* **2022**, *300*, 120720. [[CrossRef](#)]
184. Tronconi, E.; Groppi, G.; Visconti, C.G. Structured Catalysts for Non-Adiabatic Applications. *Curr. Opin. Chem. Eng.* **2014**, *5*, 55–67. [[CrossRef](#)]
185. Luisetto, I.; Sarno, C.; De Felicis, D.; Basoli, F.; Battocchio, C.; Tuti, S.; Licocchia, S.; Di Bartolomeo, E. Ni Supported on  $\gamma$ -Al<sub>2</sub>O<sub>3</sub> Promoted by Ru for the Dry Reforming of Methane in Packed and Monolithic Reactors. *Fuel Process. Technol.* **2017**, *158*, 130–140. [[CrossRef](#)]
186. Chava, R.; Purbia, D.; Roy, B.; Janardhanan, V.M.; Bahurudeen, A.; Appari, S. Effect of Calcination Time on the Catalytic Activity of Ni/ $\gamma$ -Al<sub>2</sub>O<sub>3</sub> Cordierite Monolith for Dry Reforming of Biogas. *Int. J. Hydrog. Energy* **2021**, *46*, 6341–6357. [[CrossRef](#)]
187. Sadykov, V.; Pavlova, S.; Fedorova, J.; Bobin, A.; Fedorova, V.; Simonov, M.; Ishchenko, A.; Krieger, T.; Melgunov, M.; Glazneva, T.; et al. Structured Catalysts with Mesoporous Nanocomposite Active Components for Transformation of Biogas/Biofuels into Syngas. *Catal. Today* **2021**, *379*, 166–180. [[CrossRef](#)]
188. Pauletto, G.; Vaccari, A.; Groppi, G.; Bricaud, L.; Benito, P.; Boffito, D.C.; Lercher, J.A.; Patience, G.S. FeCrAl as a Catalyst Support. *Chem. Rev.* **2020**, *120*, 7516–7550. [[CrossRef](#)] [[PubMed](#)]
189. Vita, A.; Italiano, C.; Ashraf, M.A.; Pino, L.; Specchia, S. Syngas Production by Steam and Oxy-Steam Reforming of Biogas on Monolith-Supported CeO<sub>2</sub>-Based Catalysts. *Int. J. Hydrog. Energy* **2018**, *43*, 11731–11744. [[CrossRef](#)]
190. Italiano, C.; Balzarotti, R.; Vita, A.; Latorrata, S.; Fabiano, C.; Pino, L.; Cristiani, C. Preparation of Structured Catalysts with Ni and Ni-Rh/CeO<sub>2</sub> Catalytic Layers for Syngas Production by Biogas Reforming Processes. *Catal. Today* **2016**, *273*, 3–11. [[CrossRef](#)]
191. Italiano, C.; Ashraf, M.A.; Pino, L.; Moncada Quintero, C.W.; Specchia, S.; Vita, A. Rh/CeO<sub>2</sub> Thin Catalytic Layer Deposition on Alumina Foams: Catalytic Performance and Controlling Regimes in Biogas Reforming Processes. *Catalysts* **2018**, *8*, 448. [[CrossRef](#)]
192. Zhang, Z.; Zhao, G.; Li, W.; Zhong, J.; Xie, J. Key Properties of Ni/CeAlO<sub>3</sub>-Al<sub>2</sub>O<sub>3</sub>/SiC-Foam Catalysts for Biogas Reforming: Enhanced Stability and CO<sub>2</sub> Activation. *Fuel* **2022**, *307*, 121799. [[CrossRef](#)]
193. Luneau, M.; Gianotti, E.; Guilhaume, N.; Landrivon, E.; Meunier, F.C.; Mirodatos, C.; Schuurman, Y. Experiments and Modeling of Methane Autothermal Reforming over Structured Ni-Rh-Based Si-SiC Foam Catalysts. *Ind. Eng. Chem. Res.* **2017**, *56*, 13165–13174. [[CrossRef](#)]
194. Montenegro Camacho, Y.S.; Bensaid, S.; Lorentzou, S.; Vlachos, N.; Pantoleontos, G.; Konstandopoulos, A.; Luneau, M.; Meunier, F.C.; Guilhaume, N.; Schuurman, Y.; et al. Development of a Robust and Efficient Biogas Processor for Hydrogen Production. Part 2: Experimental Campaign. *Int. J. Hydrog. Energy* **2018**, *43*, 161–177. [[CrossRef](#)]
195. Montenegro Camacho, Y.S.; Bensaid, S.; Lorentzou, S.; Vlachos, N.; Pantoleontos, G.; Konstandopoulos, A.; Luneau, M.; Meunier, F.C.; Guilhaume, N.; Schuurman, Y.; et al. Development of a Robust and Efficient Biogas Processor for Hydrogen Production. Part 1: Modelling and Simulation. *Int. J. Hydrog. Energy* **2017**, *42*, 22841–22855. [[CrossRef](#)]
196. Park, D.; Moon, D.J.; Kim, T. Preparation and Evaluation of a Metallic Foam Catalyst for Steam-CO<sub>2</sub> Reforming of Methane in GTL-FPSO Process. *Fuel Process. Technol.* **2014**, *124*, 97–103. [[CrossRef](#)]
197. Roy, P.S.; Song, J.; Kim, K.; Park, C.S.; Raju, A.S.K. CO<sub>2</sub> Conversion to Syngas through the Steam-Biogas Reforming Process. *J. CO<sub>2</sub> Util.* **2018**, *25*, 275–282. [[CrossRef](#)]
198. Tarifa, P.; Schiaroli, N.; Ho, P.H.; Cañaza, F.; Ospitali, F.; Sanghez de Luna, G.; Lucarelli, C.; Fornasari, G.; Vaccari, A.; Monzon, A.; et al. Steam Reforming of Clean Biogas over Rh and Ru Open-Cell Metallic Foam Structured Catalysts. *Catal. Today* **2022**, *383*, 74–83. [[CrossRef](#)]
199. Tu, P.H.; Le, D.N.; Dao, T.D.; Tran, Q.-T.; Doan, T.C.D.; Shiratori, Y.; Dang, C.M. Paper-Structured Catalyst Containing CeO<sub>2</sub>-Ni Flowers for Dry Reforming of Methane. *Int. J. Hydrog. Energy* **2020**, *45*, 18363–18375. [[CrossRef](#)]
200. Nguyen, T.G.H.; Tran, D.L.; Sakamoto, M.; Uchida, T.; Sasaki, K.; To, T.D.; Doan, D.C.T.; Dang, M.C.; Shiratori, Y. Ni-Loaded (Ce,Zr)O<sub>2</sub>- $\delta$ -Dispersed Paper-Structured Catalyst for Dry Reforming of Methane. *Int. J. Hydrog. Energy* **2018**, *43*, 4951–4960. [[CrossRef](#)]